NASA CONTRACTOR
REPORT

EXPLOSIVE HYPERVELOCITY LAUNCHERS

by E. T. Moore, Jr.

Prepared by
PHYSICS INTERNATIONAL COMPANY
San Leandro, Calif.
for Ames Research Center

NATIONAL AERONAUTICS AND SPACE ADMINISTRATION • WASHINGTON, D. C. • FEBRUARY 1968

NASA CR-982

EXPLOSIVE HYPERVELOCITY LAUNCHERS

By E. T. Moore, Jr.

Distribution of this report is provided in the interest of information exchange. Responsibility for the contents resides in the author or organization that prepared it.

Issued by Originator as Report No. PIFR-051

Prepared under Contract No. NAS 2-3577 by
PHYSICS INTERNATIONAL COMPANY
San Leandro, Calif.

for Ames Research Center

NATIONAL AERONAUTICS AND SPACE ADMINISTRATION

ABSTRACT

This report summarizes the analytical and experimental effort that demonstrates the feasibility of using a two-stage explosively driven light gas gun to obtain high projectile velocities. The second stage of this gun consists of an explosive lensing system that is used to produce an implosively formed piston whose velocity can be increased uniformly. The uniformly accelerated piston is shown to generate a nearly constant base pressure for projectile accelerations. Velocities as high as 12.2 km/sec have been obtained for a 0.17-gram magnesium-lithium projectile.

LIST OF KEY WORDS

1. Light Gas Guns

2. Hypervelocity Launchers

3. Hypervelocity, High Velocity

4. Explosively Driven Gas Gun
   Explosive Drivers
   Explosive Device

5. Launcher

6. Guns

7. Ballistics

8. Projectiles

9. Gas Dynamics

10. Re-entry

11. Impact

12. Hypervelocity Impact

CONTENTS

LIST OF ILLUSTRATIONS

LIST OF ILLUSTRATIONS (cont'd)

LIST OF ILLUSTRATIONS (cont'd)

SECTION I

INTRODUCTION

Many aspects of the space-exploration program involve the interaction of solid matter with gases or other solids at high relative velocities. Examples of such interactions are meteroid impact on space vehicles, planetary re-entry, and lunar cratering. In order to study these phenomena terrestrially it is necessary to have controlled laboratory means of accelerating known masses to velocities as high as 72 km/sec, depending on the particular problem to be investigated. Unfortunately, the operational velocities of such devices used to accelerate predetermined and integral aerodynamic shapes are an order of magnitude below this velocity.

For the past year Physics International has been engaged in a program of research to develop an explosively driven, light gas gun for accelerating intact projectiles of about 0.2-gram mass to the highest possible velocities. It has been recognized that the most effective launch cycle for achieving this goal would apply constant pressure to the base of the projectile for as long as possible. A constant base pressure launch cycle is also desirable from the standpoint of projectile integrity since it allows the simplest and least destructive accelerating wave system to be established within the projectile. In this situation, the maximum operational base pressure is then chosen safely below the maximum tolerable stress that the projectile material can support.

The research carried out in this program has been focused on a two-stage gun design that employs a unique explosive lensing system to provide the second-stage launch cycle. This lens processes the second-stage accelerating gas by a series of weak shocks to produce a nearly uniform projectile acceleration. Tests of this design have resulted in terminal velocities of 12.2 km/sec for a 0.17-gram metal projectile. The results

reported here represent experimental confirmation of the concepts applied in the two-stage launcher. As yet no attempt has been made to optimize the launcher system or maximize the projectile velocities. A summary of the program to develop the two-stage gun is given in Section II, with particular emphasis on the explosive lens and the second-stage launch cycle.

In support of the work on explosively driven launchers, a comprehensive experimental investigation was undertaken to determine the performance characteristics of explosive drivers. As a result of this study, three phenomena have been incorporated in a model of explosive-driver operation to account for observed departures from the ideal driver behavior (Section III). They are: (1) radial expansion of the gas-containing pressure tube, (2) the effect of boundary-layer growth in the driver, and (3) the formation of a metal, gas, or metal-gas jet by the progressively collapsing pressure tube. Although this investigation was carried out using linear explosive drivers, the results are qualitatively applicable to any system in which a piston is formed by the collapse of a gas-containing tube. The results of this study are summarized in detail in Section IV.

SECTION II

TWO-STAGE EXPLOSIVELY DRIVEN LAUNCHERS

The two-stage launching system is designed around a unique explosive lensing system that is used to collapse a gas-filled tube in a prescribed manner. The progressive collapse may be represented as a piston propagating into the gas with a velocity equal to the detonation velocity of the explosive that surrounds the tube. The velocity of such a piston can be changed almost instantly. For the launching system initially investigated, the explosive lens used as the second stage was designed to form a piston that accelerated uniformly. The operation of this lensing system is shown schematically in Figure 1.

Detonation velocity along the outside of the tube is $V_1 = D_1$ from A to B and then increases uniformly to $V_2 \gg V_1$ from B to C.
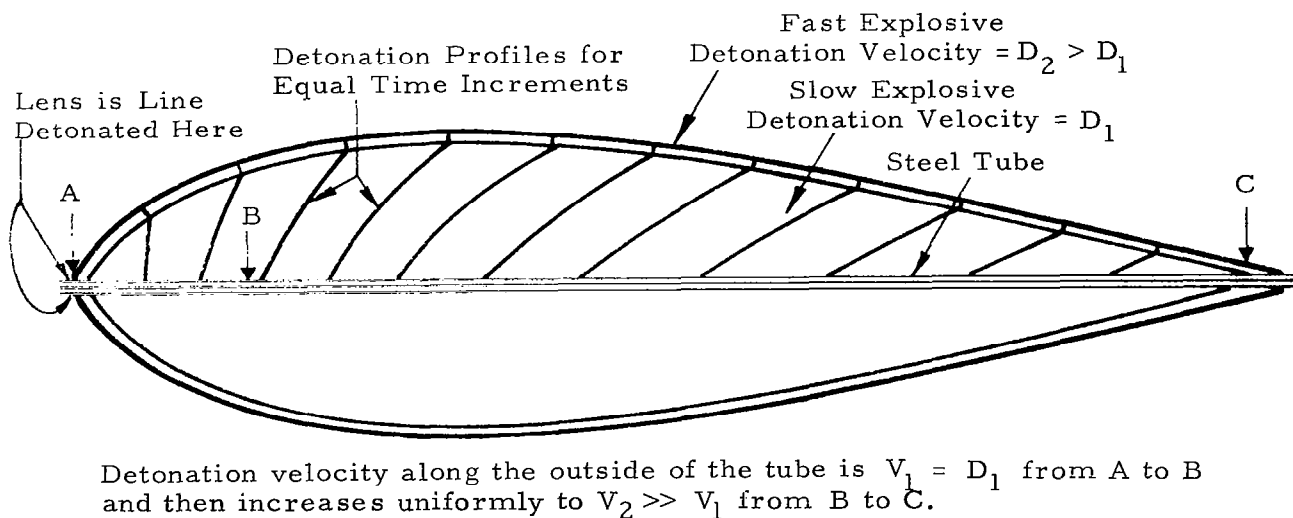
FIGURE 1. UNIFORM ACCELERATION EXPLOSIVE LENS

After the lens is initiated, a detonation wave front proceeds along the steel tube with a velocity that is initially equal to the detonation velocity of the slow explosive. However, the combination of the higher detonation velocity in the fast explosive and the changing contour of the interface

between the fast and slow high explosives produces a continuously tilting wave front, or a phased detonation wave. As a result, the piston formed by the collapse of the steel pressure tube begins to accelerate. In general, the lens can be made to yield extremely high piston velocities. Yet there is an upper limit at which the collapsing tube will no longer drive the gas ahead of it, and this limit can be determined only by experiments. It now appears that 20 km/sec is a reasonable value to assume for this upper limit.

An inherent limitation on explosive drivers in general and the explosive lens in particular is the lowest velocity limit imposed on the piston. The minimum piston velocity corresponds to the slowest detonation velocity employed in the lens. While there are high explosives with detonation velocities as low as 2 km/sec (Reference 1), tests have shown that 5 km/sec represents a more realistic lower limit because of the energy density of the explosive that is required to properly collapse a metal tube. This lower velocity limit requires that a first-stage launcher be used to inject the projectile and a sufficient length of driver gas into the second-stage explosive lens at a velocity in the neighborhood of 5 km/sec. Figure 2 shows schematically the collapse of the first-stage barrel and the formation of a conical piston after the second-stage lens has been partially detonated.
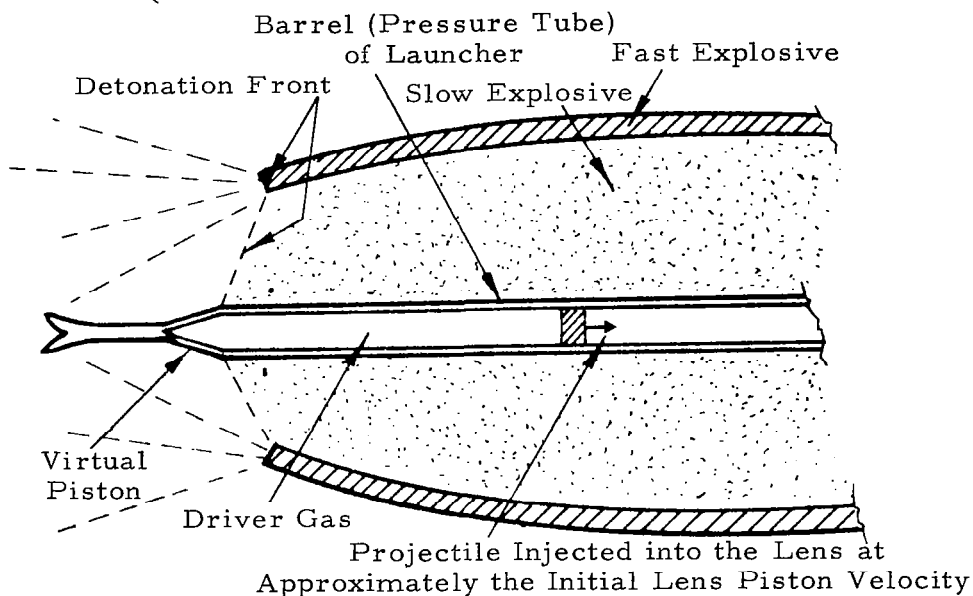
FIGURE 2. OPERATION OF EXPLOSIVE LENSING SYSTEM

The operation of a complete two-stage launching system is illustrated in Figure 3. The first stage is a tamped[*] linear explosive driver, which accelerates the projectile from rest by reflecting a strong shock from the base of the projectile. The first stage is long enough so that the rarefaction produced when the first-stage piston is stopped does not significantly affect the driver gas injected into the second stage. The operation of the explosive lens is initiated by a trigger pin that responds to the arrival of the first-stage shock wave at the chambrage plane. When the projectile and the driver gas have been accelerated by the first stage to approximately 5 km/sec, the second-stage piston is formed and begins to accelerate uniformly. The acceleration of the second-stage piston is programmed so that the peak pressures generated on the base of the projectile are maintained below a certain specified limit during the launch cycle. For this design, the second-stage piston is accelerated uniformly to 12 km/sec, at which point it is stopped. The projectile continues to accelerate to its terminal velocity of 14.1 km/sec by the expansion of the second-stage driver gas.

A. FIRST-STAGE ACCELERATION

The gasdynamic cycle of the first stage is accomplished by a linear tamped explosive driver using helium as the driver gas. The tamper minimizes the radial expansion of the pressure tube behind the shock wave and makes it possible to obtain longer lengths of shocked gas. However, arbitrarily long lengths of shocked gas were found to be impossible because of the growth of a boundary layer in the shocked gas. Since the gas in the boundary layer receives little additional axial acceleration from the implosion of the gas-containing pressure tube, it is left behind the detonation wave and trapped by the collapsing tube. This loss of gas causes downstream-running rarefaction waves that reduce the pressure and velocity of the shocked

---

[*]A thick-walled metal tube, the tamper, surrounds the explosive and is designed to minimize the radial expansion of the pressure tube behind the shock wave.

Diluted Nitromethane
D = 5.5 km/sec

Detasheet
D = 7.6 km/sec

Helium
245 psi

Nitromethane
D = 6.4 km/sec

Projectile

First Stage Tamped
Linear Explosive Driver

Second Stage
Explosive Lens

Detonator

a. Initial Configuration

Detonation Wave

Shock

Constant-Velocity
Virtual Piston

Helium ~ 2 kb

b. First-Stage Linear Driver Operation

Reflected Shock and
Detonation About to Meet

Helium 8 kb

Phased
Detonation Wave

c. Second Stage Initiated: Projectile and Driver Gas
Being Injected into Explosive Lens

Phased
Detonation Wave

Accelerating
Virtual Piston

d. Explosive Lens Accelerates Projectile to Final Velocity
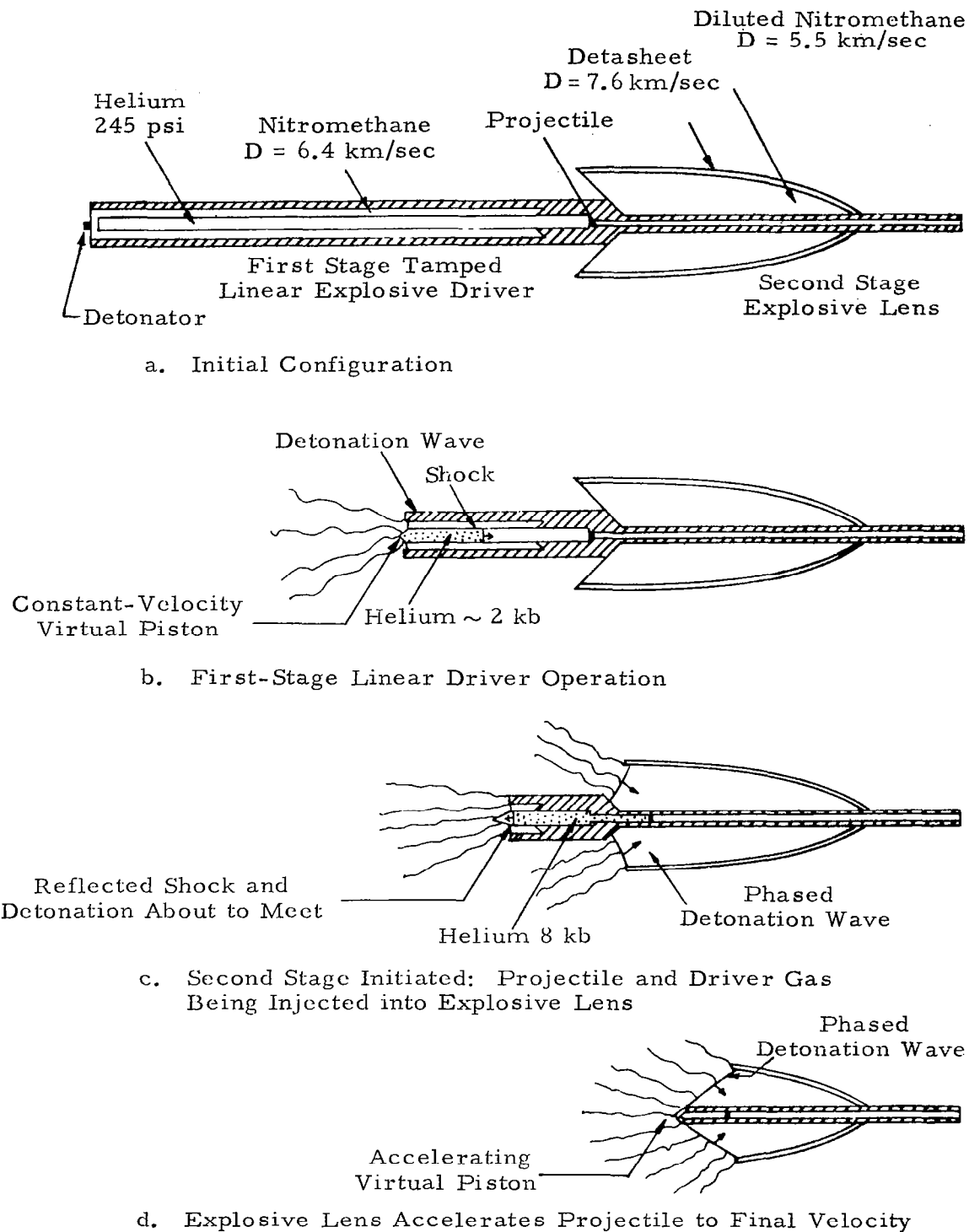
FIGURE 3. OPERATION OF A TWO-STAGE EXPLOSIVELY
DRIVEN LAUNCHER

6

gas and decrease the shock velocity. This loss continues until the mass flow through the shock wave equals the mass flow trapped by the collapsing liner. At this point, the shock velocity becomes equal to the piston velocity, and the length of shocked gas reaches a fixed steady-state value.

It was necessary to know the precise acceleration history of the projectile as well as the time-space variation of driver-gas properties in the first stage in order to determine when and where the second-stage operation should begin. Therefore the effects of boundary-layer growth in the first-stage driver had to be accounted for in any calculation of first-stage performance. Based on observed driver performance, a method of calculation was devised to account for these gas conditions in the first-stage driver. The method is reported in detail in Section IV.

The performance calculation of the first-stage driver was carried out using a one-dimensional, hydrodynamic computer program capable of simulating area changes. In the calculation, an 0.25-inch-diameter, 0.17-gram projectile having an areal density of 0.5 gm/cm^2 was accelerated into air at one atmosphere. After accelerating for 60 cm the velocity of the projectile was 5.2 km/sec, and the base pressure and counterpressure were virtually equal. The results of this calculation are shown in Figure 4. Included in this figure are several relevant pressure distributions taken at various times during the acceleration of the projectile.

In the course of the reproducibility tests of the first-stage launcher, a new diagnostic technique was developed to experimentally measure the position-time history of the accelerating projectile in the barrel. This technique utilized a high-speed streaking camera to record the passage of the air shock, the projectile, and the hot-helium driver gas by viewing through small apertures in the barrel (see Figure 5). These apertures were filled with clear glass rods to delay any small rarefactions that would
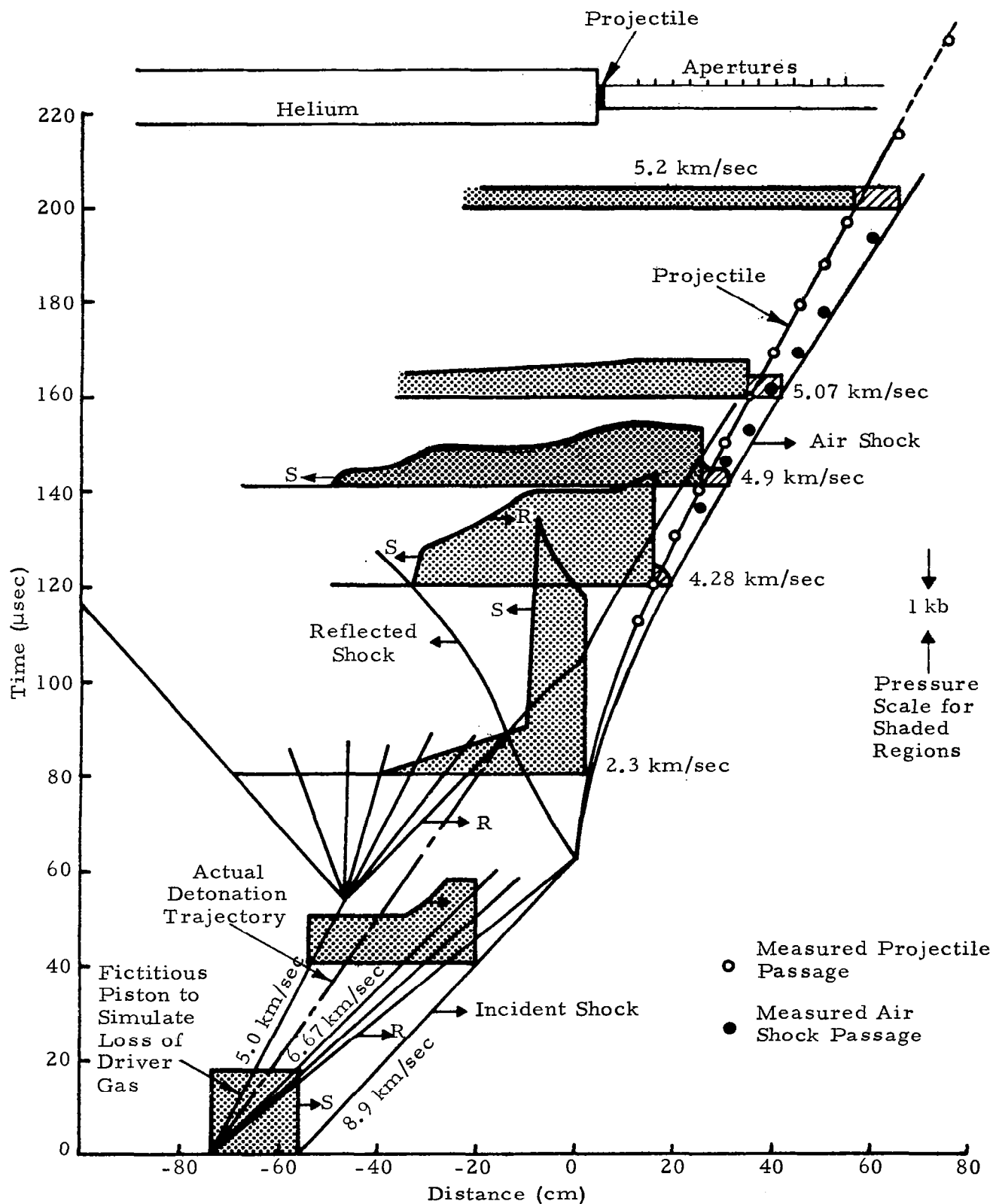
FIGURE 4. COMPUTED AND EXPERIMENTAL PERFORMANCE OF
FIRST STAGE OF A TWO-STAGE LAUNCHING SYSTEM

First Aperture
at 12.5 cm

Muzzle

Projectile Emerging
from Gas Cloud

Timing Bridgewire

Projectile

Air Shock

Breech and Muzzle
Timing Bridgewires

Explosive Candle
Back-Lighting

Time

Distance
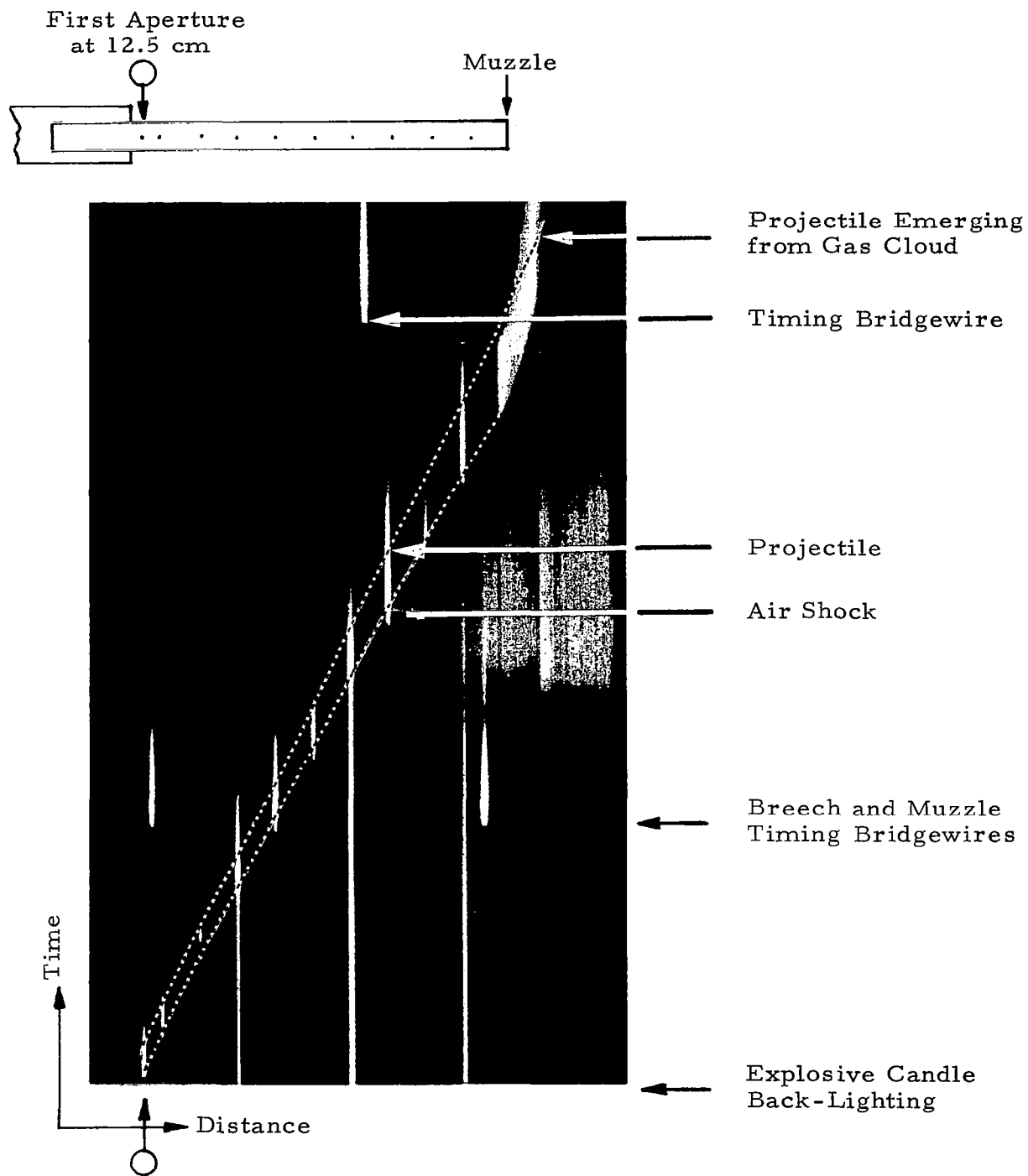
FIGURE 5. STREAKING RECORD OF PROJECTILE
ACCELERATING WHILE IN GUN BARREL
(Shot LRG-4)

modify the pressure distribution behind the projectile. An experiment was designed using experimental parameters identical to those used in the above performance calculation. The projectile was launched intact to a velocity of 5.4 km/sec. A range radiograph of the projectile in flight is printed as Figure 6. The observed trajectory of the projectile in the barrel was
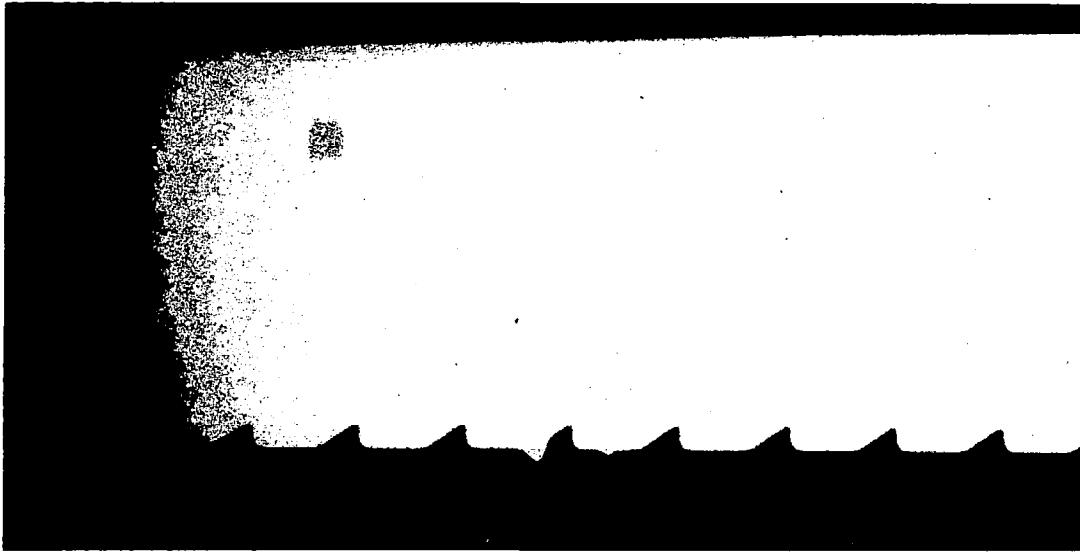
FIGURE 6. RANGE RADIOGRAPH OF PROJECTILE
ACCELERATED BY A FIRST-STAGE LAUNCHER

almost identical to the calculated trajectory. The detailed comparison of the experiment and the calculation is shown in the time-distance plane of Figure 4. Since the agreement of the calculated with the observed performance of the first-stage launcher was excellent, the calculated pressure, density, and velocity distributions of the gas behind the accelerating projectile were assumed to be quite close to the actual gas-dynamic conditions. The ability to calculate the first-stage projectile acceleration in detail is vital to the operation of the two-stage system. Because of the microsecond time scale, it is necessary to know very closely the time at which conditions in the first stage are optimum for the operation of the second stage to begin.

B. SECOND-STAGE ACCELERATION

The explosive lens used in the second-stage accelerates the projectile from about 5 km/sec to the desired final velocity. For the purposes of initial tests, the lens was designed to produce a uniformly accelerating piston. Because of the communication time between the accelerating piston and the projectile, there will always be shock waves reflecting between the piston and the projectile. By properly matching the piston acceleration to the driver-gas conditions and the areal density of the projectile, these shocks can be made very weak.

To illustrate this point, several calculations of second-stage performance were made. Each calculation was based on the gas conditions and the projectile velocity chosen from the first-stage performance calculation (Figure 4). That is, the second-stage piston would be formed 10 cm downstream of the chambrage plane (or area change) at the time when the projectile is moving at 4.8 km/sec. At this instant, there is 15 cm of driver gas at approximately 1.3 kb between the piston and projectile. The calculated pressure distribution behind the projectile at this time is shown in Figure 7.

In order to produce a nearly constant base pressure, it is necessary to choose the second-stage acceleration a that is equal to the ratio of the pressure P in the driver gas at the time the second-stage acceleration begins to the areal density σ of the projectile and driven gas; or, $a = \frac{P}{\sigma}$. The calculated position-time history given in Figure 8a illustrates the performance of a second-stage acceleration that is matched to the first-stage gas conditions in this manner. For this calculation, the second-stage piston accelerates uniformly from 5.5 km/sec to 12 km/sec over a distance of 280 cm. Figure 8b shows the nearly constant base pressure produced by this acceleration.
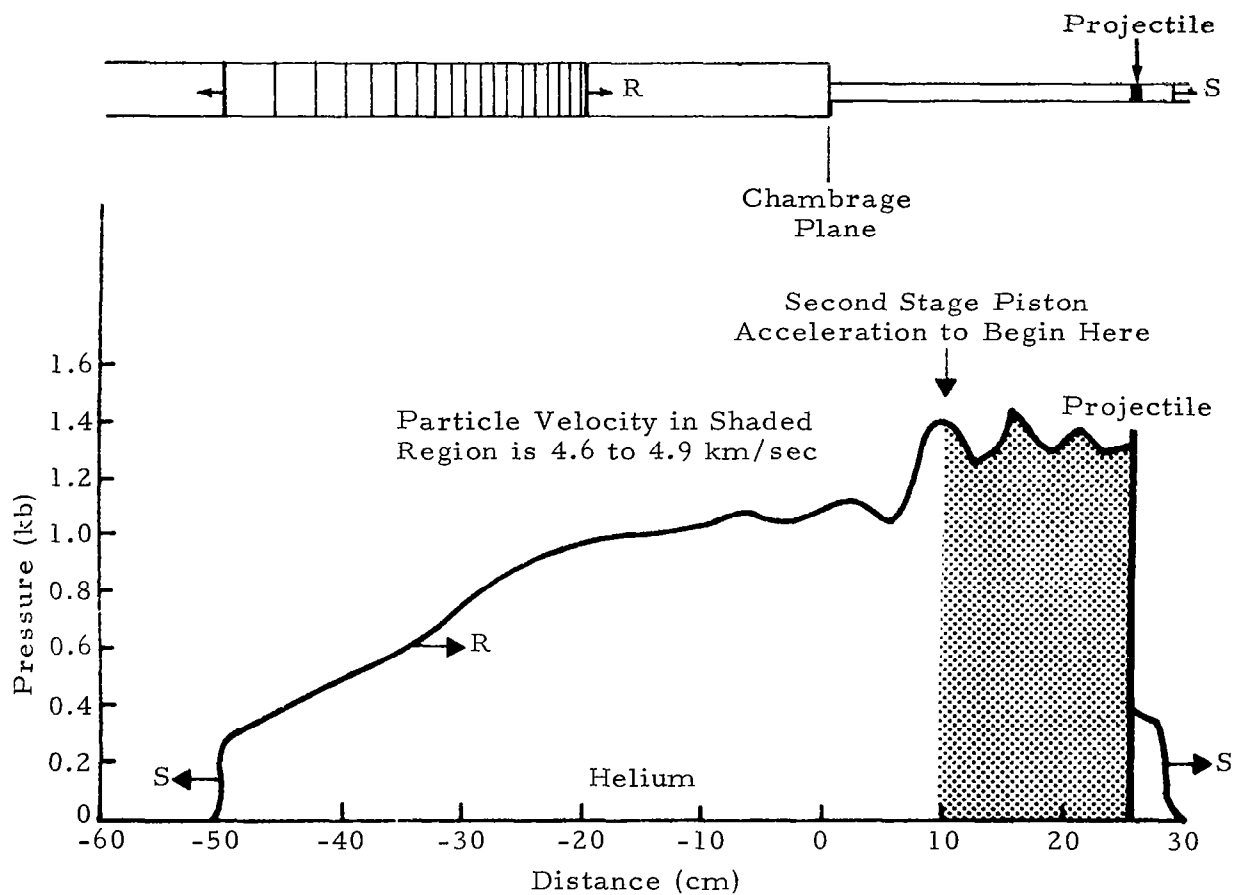
FIGURE 7. COMPUTED PRESSURE DISTRIBUTION BEHIND THE
PROJECTILE AT THE TIME THE SECOND-STAGE
ACCELERATION IS INITIATED, WHEN PROJECTILE
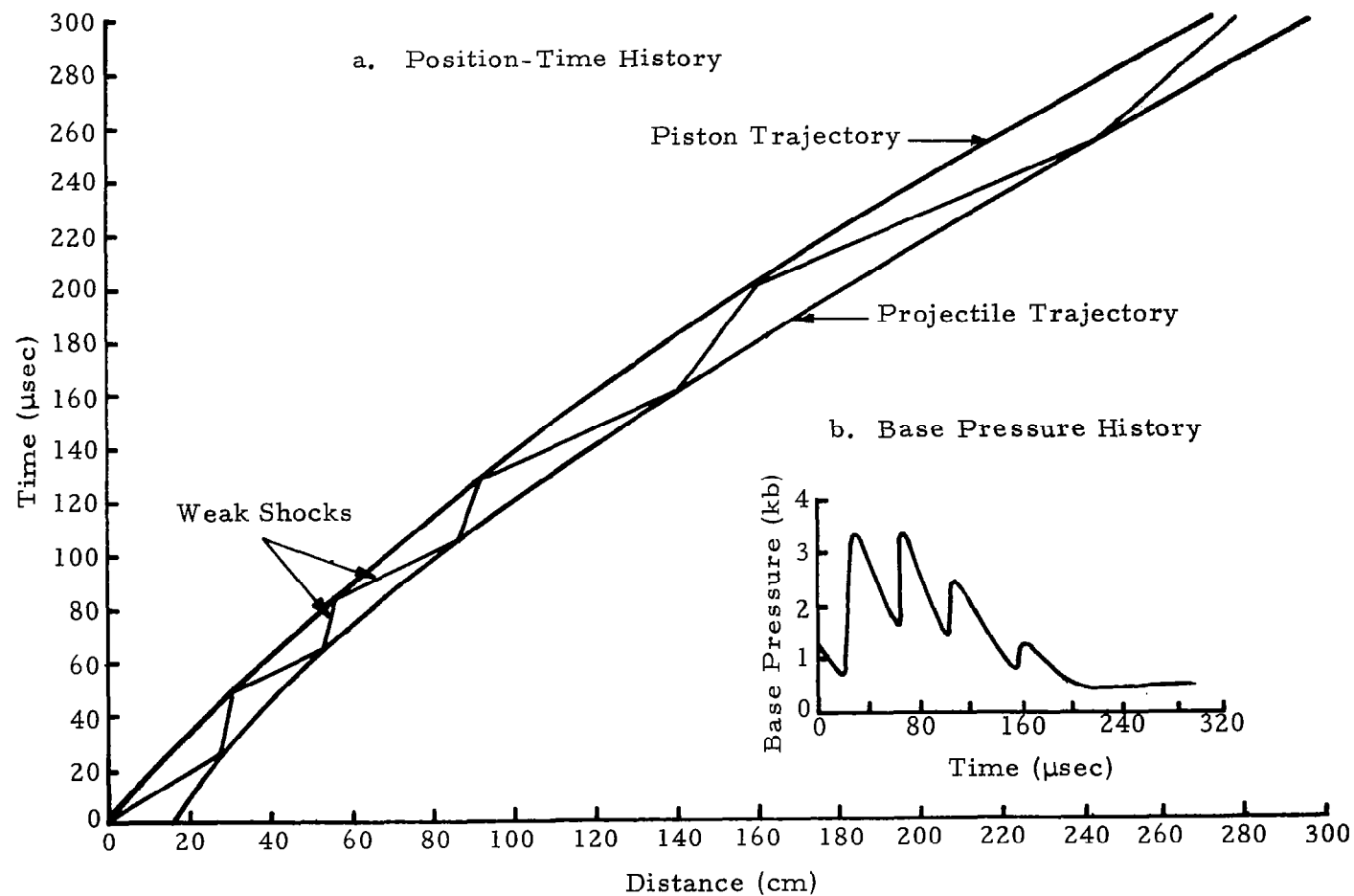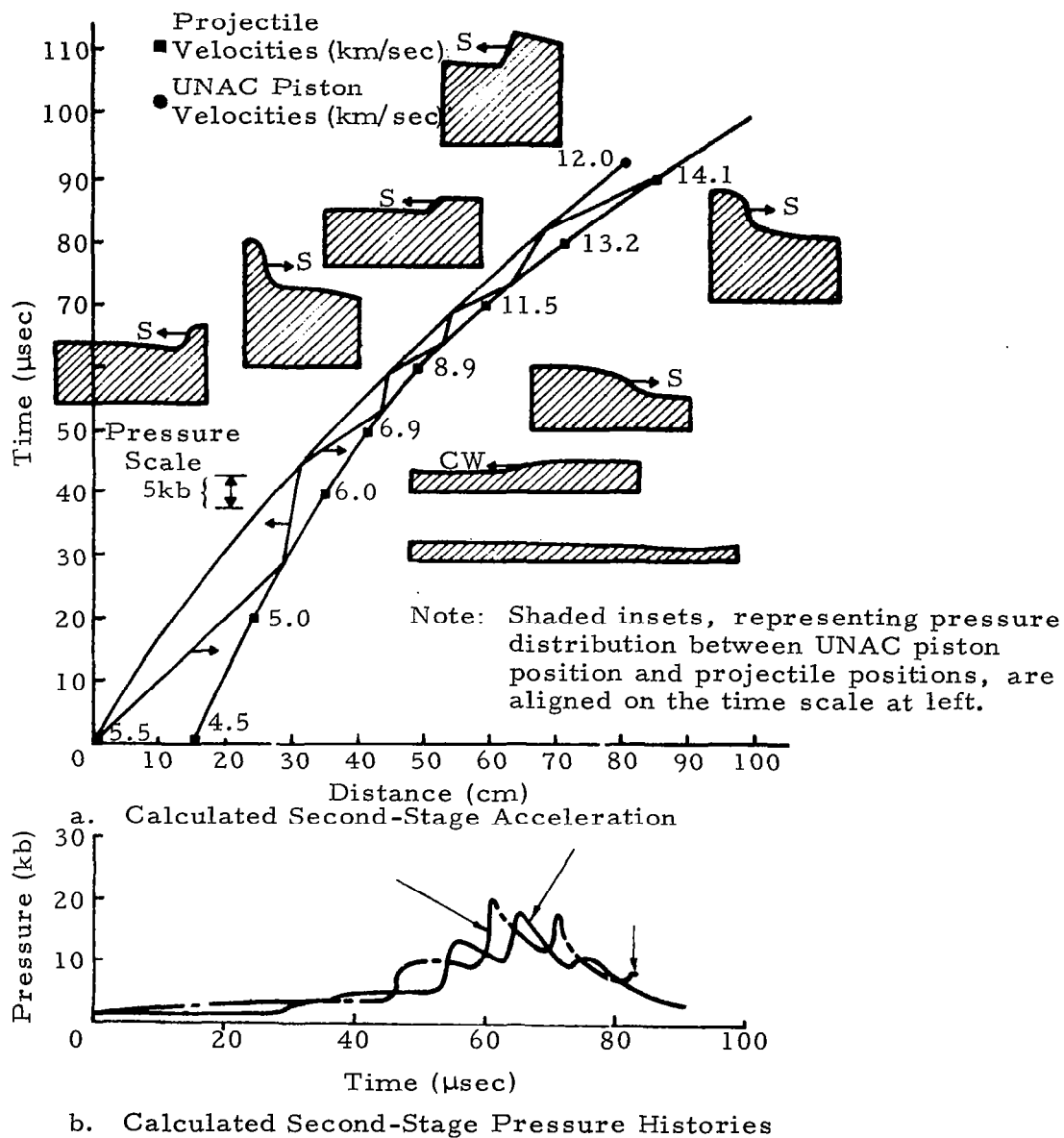VELOCITY = 4.9 km/sec

FIGURE 8. CALCULATED PERFORMANCE OF A SECOND-STAGE
ACCELERATION MATCHED TO THE GAS CONDITIONS
GENERATED BY THE FIRST STAGE

While the above calculation represents the most desirable type of launching cycle, the 280-centimeter explosive lens that would be required to reach projectile velocities in the neighborhood of 15 km/sec presented certain fabrication difficulties. The alternative would be to redesign the first-stage launcher to permit the use of a shorter explosive lens. In order to expedite the fabrication, assembly, and test of a two-stage explosively driven launcher, additional calculations were made to examine uniform second-stage acceleration that did not match the driver-gas conditions generated by the first stage.

In the first calculation, the piston accelerated uniformly from 5.5 km/sec to 12 km/sec over a distance of 41 cm. The results showed that the projectile reached a final velocity of 14.5 km/sec. However, the peak base pressures generated by this launch cycle were over 70 kb, and this represented an intolerable environment for both the projectile and the explosively formed piston.

In the second calculation, given in Figure 9, the piston accelerated uniformly from 5.5 km/sec to 12 km/sec over 82 cm, or one-half the acceleration of the previous calculation. Peak pressures of only 20 kb were produced in this launch cycle and the projectile was accelerated to 14.1 km/sec. Since saboted models have been launched at peak pressures of 24 kb (Reference 2), this piston acceleration not only represented a practical launch cycle, but it was also one in which the peak pressures and detailed wave interactions were compatible with the integrity of the projectile. As a result, this acceleration was chosen to test the uniformly accelerated, explosive lensing concept.

To determine the sensitivity of launcher performance to the exact time at which the second-stage lens is initiated, two additional performance calculations were made. In each calculation the second-stage piston

a. Calculated Second-Stage Acceleration

Note: Shaded insets, representing pressure distribution between UNAC piston position and projectile positions, are aligned on the time scale at left.

b. Calculated Second-Stage Pressure Histories

Note: Areal Density of Projectile is 0.5 gm/cm^2

FIGURE 9. CALCULATED PERFORMANCE OF THE SECOND STAGE FOR AN 82-centimeter EXPLOSIVE LENSING SYSTEM

accelerated from 5.5 km/sec to 12.0 km/sec over a distance of 82 cm. The gas conditions for the first calculation were taken from the first-stage performance calculations assuming the second-stage lens was initiated 10 μsec early. In a similar manner the gas conditions for the second calculation simulated the feasibility that the second lens was initiated 10 μsec later than desired. The results indicate that early initiation of the second stage results in lower peak pressures on the projectile and piston, but the final velocity is also slightly lower (13.2 km/sec). If the second-stage initiation is late, there is not substantial change in the peak pressure generated or the final velocity of the projectile. In all three design cases, the muzzle exit times were approximately the same.

The calculated performance of the complete two-stage launching system is shown in Figure 10.

C.   SECOND-STAGE EXPLOSIVE LENS

The most effective second-stage lens design is dictated by two requirements: (1) The piston should begin to accelerate from the lowest possible velocity, which is determined by the detonation velocity of the slow explosive component. (2) For a given piston acceleration, the maximum economy of explosives is obtained for the greatest difference in the detonation velocities of the fast and the slow explosive components.

Nitromethane represented a very practical choice for the slow component since it is an inexpensive liquid explosive with sufficient energy density to properly collapse a metal tube. Also, it is a homogeneous liquid explosive that provides uniform detonation characteristics, which reduces dimensional tolerances. Several tests were made to determine the lowest detonation velocity that could be obtained by diluting nitromethane with methyl alcohol. In each of these tests the mixtures were sensitized with 5 percent by volume of ethylene diamine. The results of these tests are
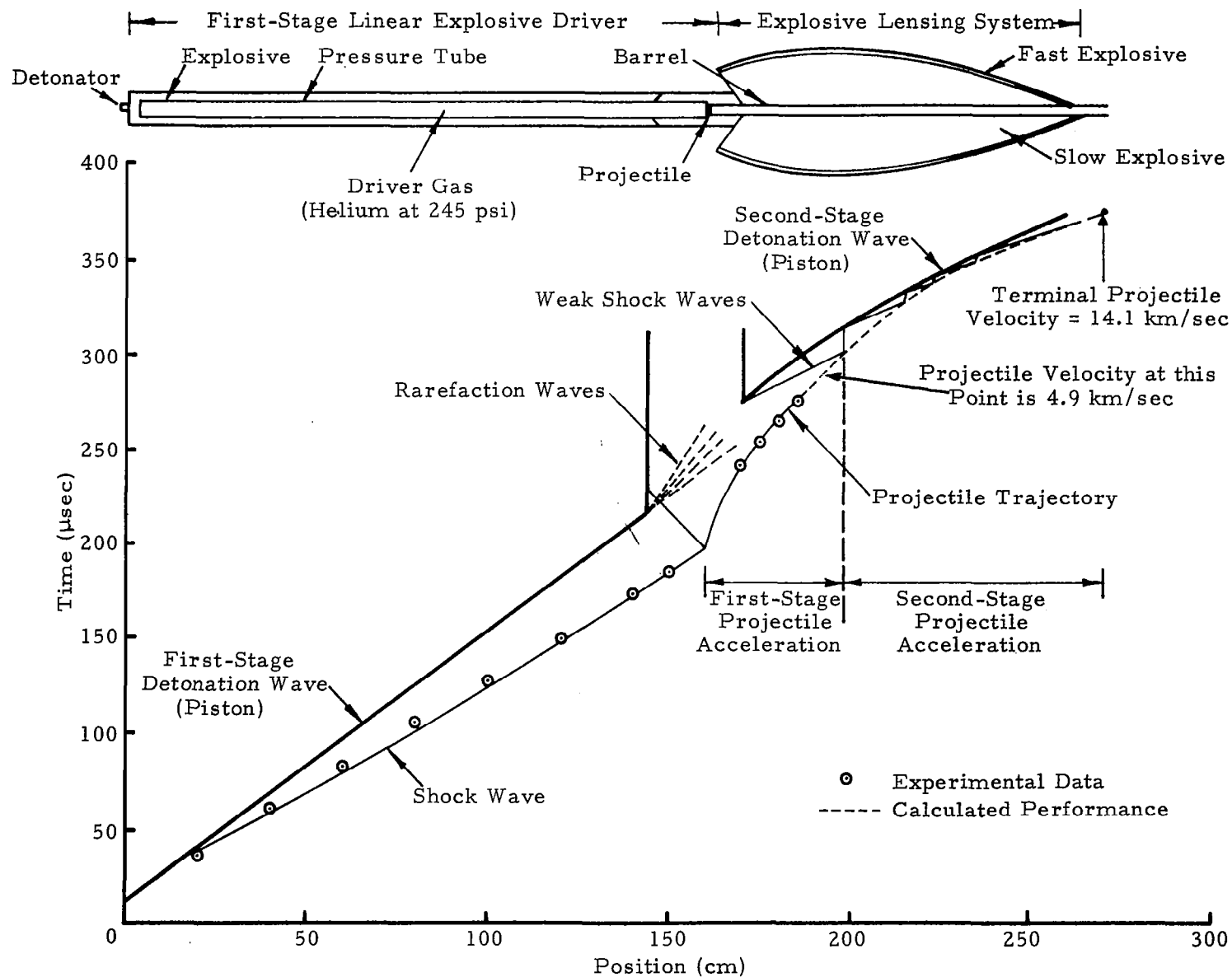
FIGURE 10. PERFORMANCE OF A COMPLETE TWO-STAGE
EXPLOSIVELY DRIVEN, LIGHT GAS GUN

shown in Figure 11.   It was found that a mixture containing 45 percent by volume of methyl alcohol, whose detonation velocity was 4.9 km/sec, represented the threshold of stable detonation.   A mixture of 30 percent methyl alcohol by volume whose detonation velocity is 5.5 km/sec was then selected as the slow explosive component of the lens since it was well within the limits of a stable, reproducible detonation.
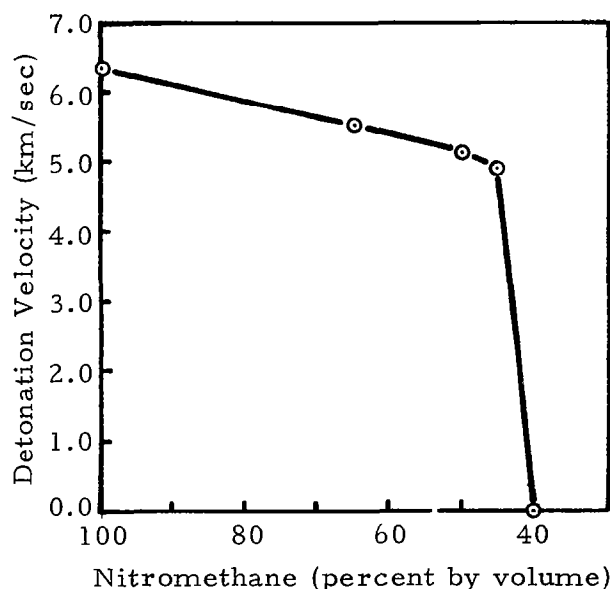
Note: Mixture Contained in Steel Tube,
0.5625-inch I. D.   x 0.875-inch O. D.

FIGURE 11.   DETONATION VELOCITY OF NITROMETHANE DILUTED
WITH VARIOUS AMOUNTS OF METHYL ALCOHOL

Besides having a high detonation velocity, the fast explosive component of the lens must be compatible with the geometry and containment of the diluted nitromethane.   For these reasons Dupont Detasheet (EL506A8) was chosen as the fast explosive component.   This commercial explosive is composed of an integral mixture of PETN (pentaerythritol tentranitrate) and elastomer binder and has a detonation velocity of 7.7 km/sec.   Since Detasheet is available in sheets of various thicknesses which may be cut to the desired configuration and bonded to almost any surface, it is well suited for the contour of the lens.

18

Tests were then conducted to determine the ability of Detasheet to initiate diluted nitromethane through the polyvinyl chloride used to contain the diluted nitromethane. Polyvinyl chloride (PVC Type I) is a thermal plastic selected because of its ability to be formed into arbitrary shapes and its resistance to corrosion by nitromethane. In order to determine the thickness of PVC through which the Detasheet would initiate the nitromethane, an experiment was conducted in which a PVC wedge separated the two explosives as in Figure 12. The results showed that Detasheet could initiate the nitromethane through 0.080 in. of PVC. Consequently, all the lens contours have been fabricated from PVC in thicknesses ranging from 0.030 in. to 0.060 in. An interesting by-product of this experiment should be noted: as the shock wave progressed from the thick to the thin end of the wedge, the shocked but undetonated nitromethane changed color from a light yellow to a deep red. The spectrum did not represent a self-sustaining chemical reaction, but it appeared to follow pressure fluctuations in the liquid. It is possible that this effect could be developed as a technique for measuring transient high pressures.

A prototype lens for testing the accuracy of the programmed piston acceleration and the lens's ability to produce an accelerating shock wave was constructed using a vacuum-forming technique. It was designed to provide a uniform piston acceleration from 5.5 km/sec to 12.5 km/sec over a distance of 60 cm. Its 1.5-inch-diameter pressure tube initially contained helium at 410 psi. Shorting pins, piezoelectric transducers, and a resistance-wire gauge along the pressure tube monitored the detonation and shock trajectories. The results of this test are shown in the time-distant plane of Figure 13. The predicted and the observed detonation trajectories coincide, and the shock wave does accelerate. There is evidence of jetting in the implosively formed piston since the observed shock breaks out faster than predicted, but this behavior can be minimized or eliminated by the proper choice of experimental parameters.
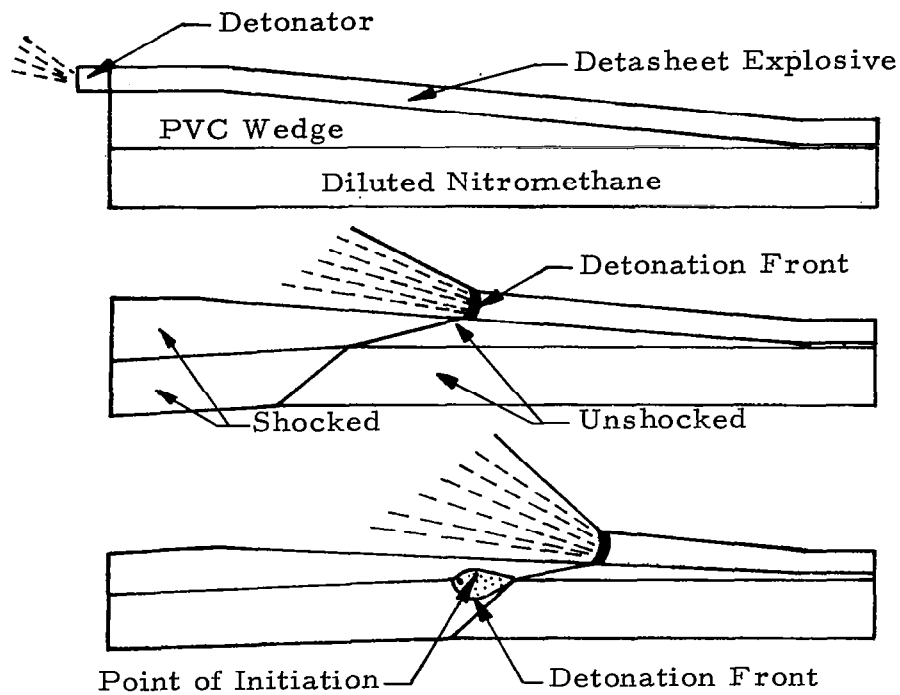
a. Schematic Representation of Experiment
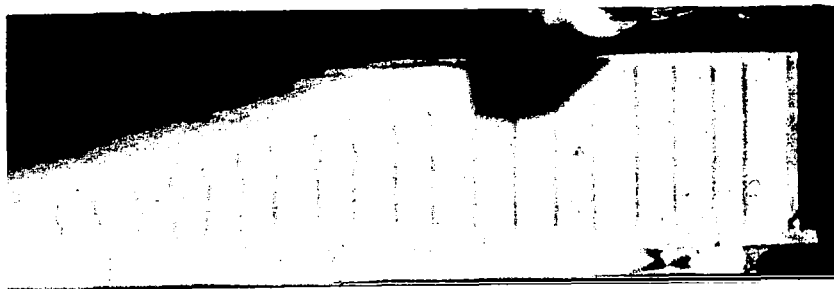
b. Framing Camera Photograph Showing Detonation
   Wave in Diluted Nitromethane at a PVC Thickness
   of ~ 0.80 inches

FIGURE 12.   EXPERIMENT TO DETERMINE THE MINIMUM
             THICKNESS OF POLYVINYL CHLORIDE (PVC)
             THROUGH WHICH DuPONT DETASHEET (EL506A8)
             CAN INITIATE DILUTED NITROMETHANE

Detasheet
Detonation Velocity = 7.6 km/sec

Piezoelectric
Transducers

Helium (410 psi)

Detonation

Steel Pressure Tube

Diluted Nitromethane
Detonation Velocity = 5.5 km/sec

Detonation Wave

Acceleration Starts

Shock Wave

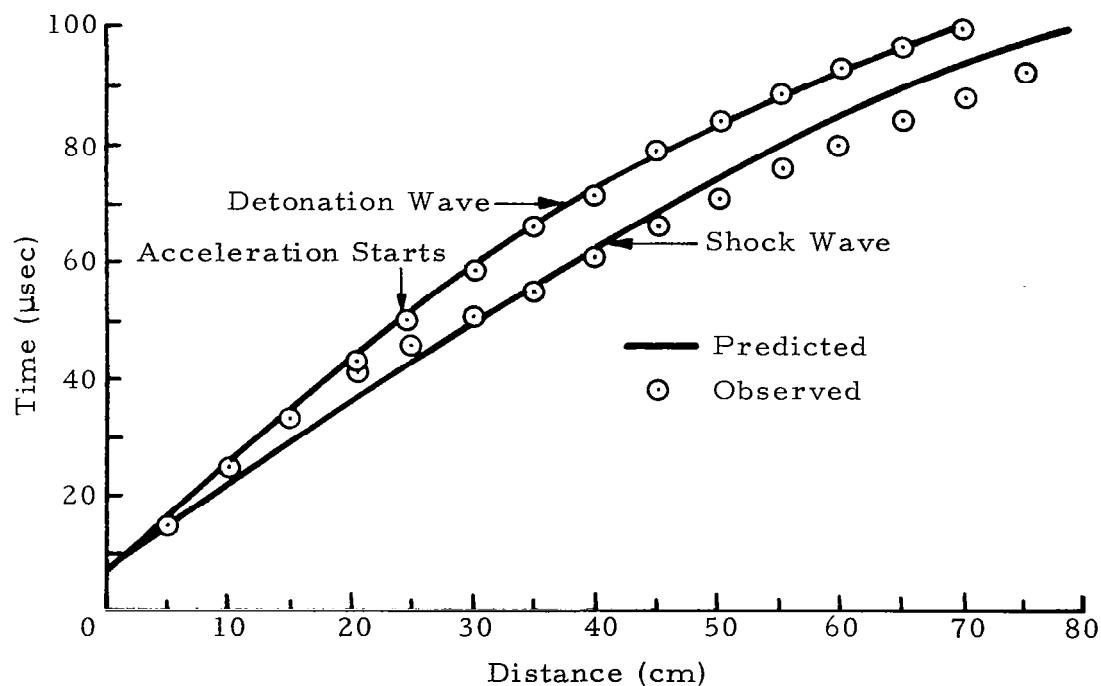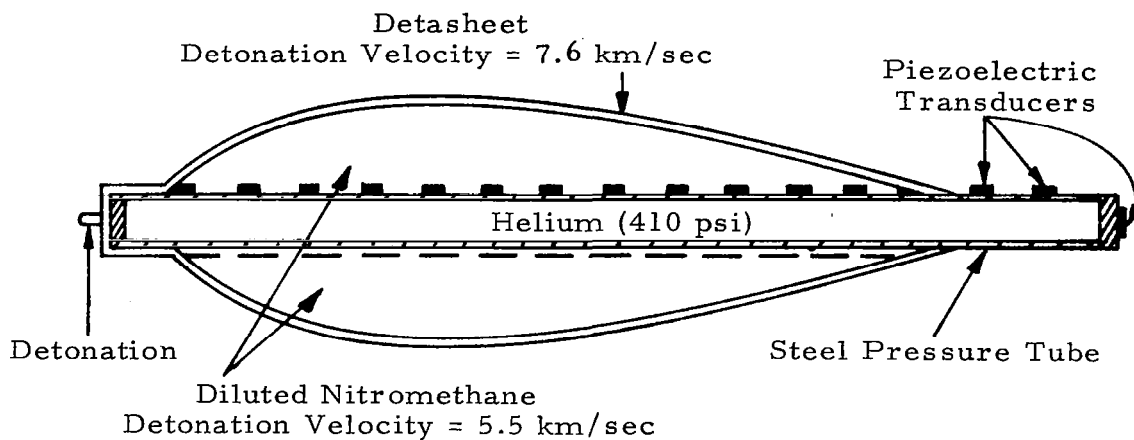Predicted

⊙ Observed

Time (μsec)

Distance (cm)

FIGURE 13.   DETONATION AND SHOCK-WAVE TRAJECTORIES
PRODUCED BY A UNIFORMLY ACCELERATING
EXPLOSIVE LENS

21

The operation of an explosive lens was further demonstrated by the experiment illustrated in Figure 14. The continuously tilting detonation wave in the nitromethane was observed experimentally by backlighting a cross-section version of the explosive lens with an explosive argon candle. The high-speed framing camera sequence given in Figure 15 shows the results of this experiment. The position-time history of the observed detonation wave plotted in Figure 15b shows that the axial component of the detonation velocity followed the programmed acceleration very precisely.

These tests established the feasibility of the explosive lens concept, but several important problems were raised. For instance, it was not clear what effect the changing mass ratio of explosive to pressure tube (c/m) of the lens had on the collapse process; in a typical lens, this c/m ratio ranges from approximately 20 to very nearly zero because of the continuously varying contour. Also, there seemed to be a relation between jetting phenomena and the ratio of pressure tube wall thickness to internal diameter. These effects were investigated in detail and the results are given in Section IV.

D. ASYMMETRIC IMPLOSION TECHNIQUE

The fabrication of a large, second-stage lens is laborious and requires a complex vacuum-formed mold for each lens contour design. This prompted a search for a simpler approach. It was postulated that the implosion process used to form the virtual piston need not be symmetric. An experimental study initiated under a separate program (Air Force Contract AF40(600)-1129) demonstrated the potential of an asymmetric implosion. Several experiments were conducted in which a metal pressure tube placed on a steel plate was collapsed asymmetrically by a tilting detonation wave that formed a constant-velocity virtual piston. The geometry of this asymmetric linear driver is shown schematically in Figure 16. The performance of the asymmetric driver was found to be quite comparable to the performance of the symmetric

Plexiglas Wall

Plexiglas Base

Electrical Pin Switches

Reference Grid

Detasheet Explosive

PVC Separator
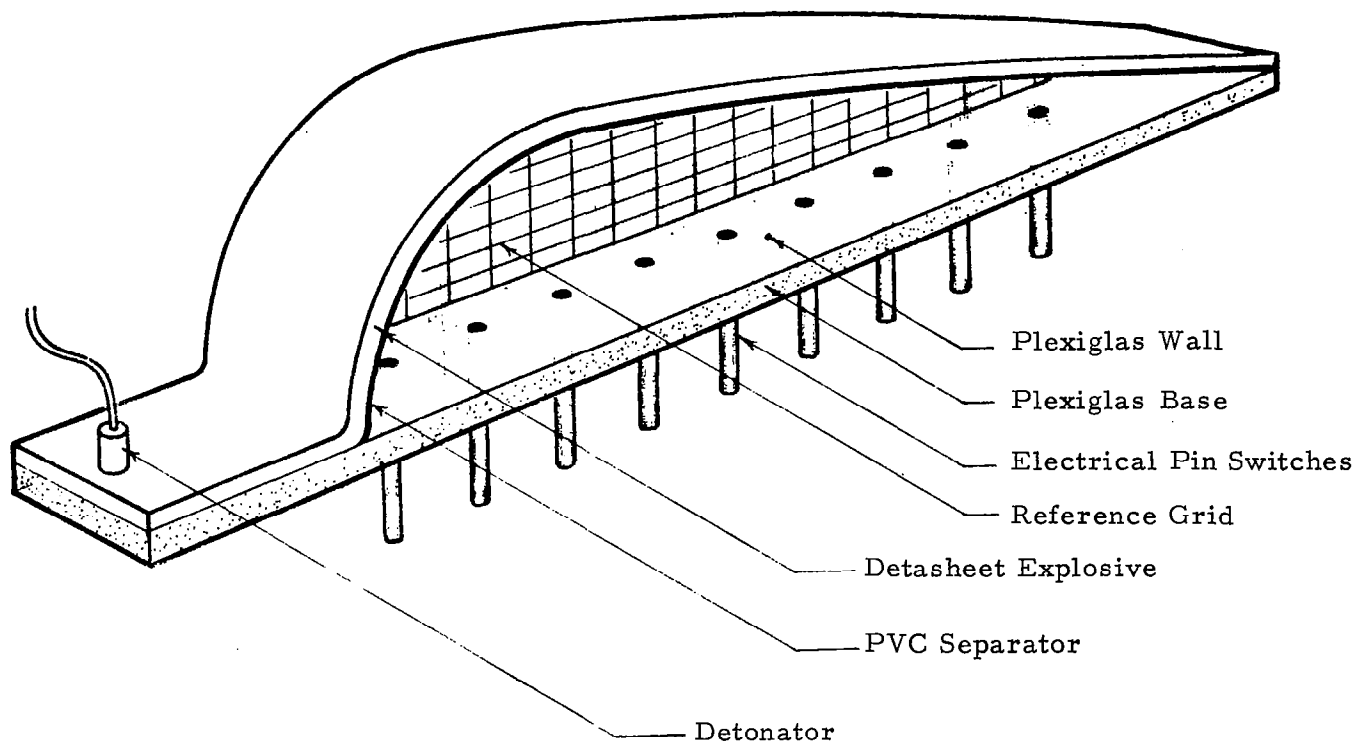
Detonator

FIGURE 14. INITIAL CONFIGURATION OF AN EXPERIMENT TO VERIFY OPERATION
OF AN EXPLOSIVE LENS (SHOT 255-1)

Time = 0

Time = 40 μsec

Time = 60 μsec
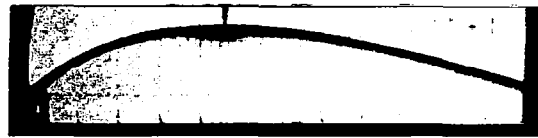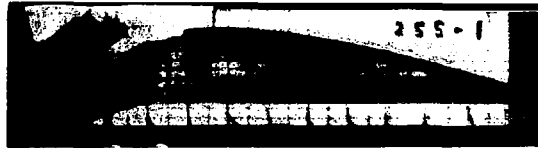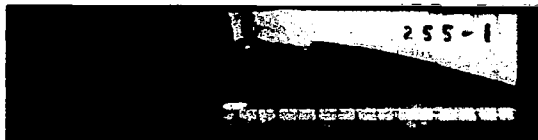
Time = 80 μsec
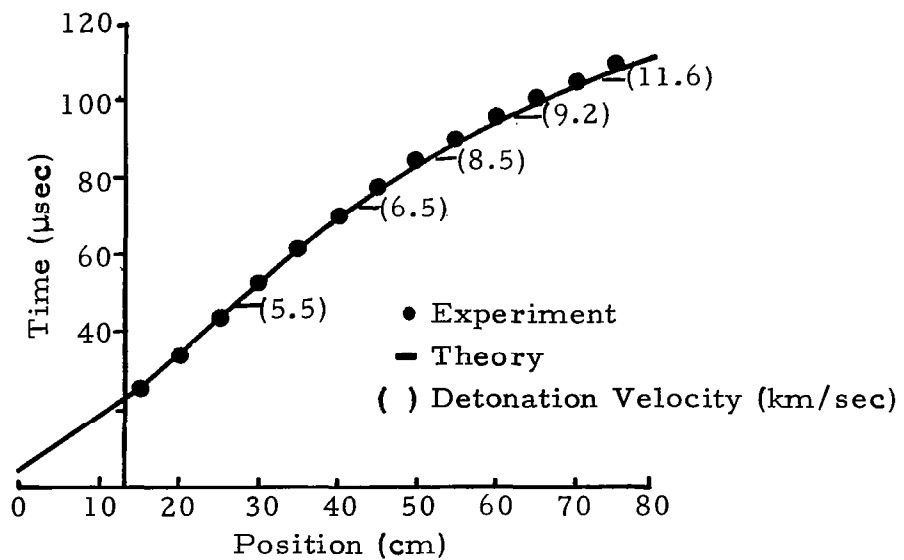
FIGURE 15.   FRAMING CAMERA SEQUENCE AND AXIAL
DETONATION VELOCITY OBTAINED FROM
EXPLOSIVE LENS EXPERIMENT ILLUSTRATED
IN FIGURE 14
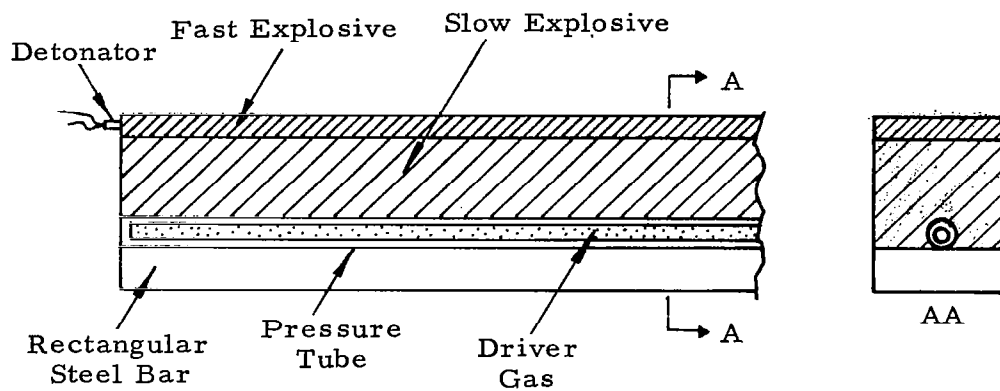
a. Before Initiation of Explosives
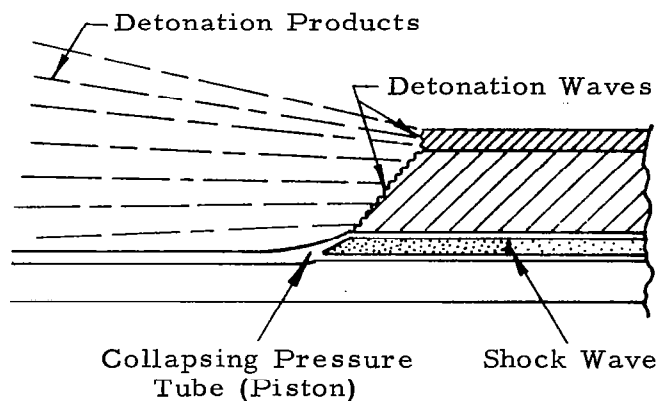
b. After Initiation of Explosives

Note: Explosive combination gives tilted detonation wave
similar to that used in explosive lens, but in this
case it does not accelerate.

FIGURE 16.   OPERATION OF AN EXPLOSIVE DRIVER UTILIZING
AN ASYMMETRIC IMPLOSION

driver. That is, the shock trajectories were found to be quite similar over the driver lengths tested.

An explosive lens contour that would provide the second-stage piston for the two-stage gun was used to fabricate a lens that would collapse a pressure tube asymmetrically. This asymmetric lens is essentially a slice of one half of the symmetric lens. The performance of this lens is shown in the high-speed framing camera record in Figure 17. The arrival times of the phased detonation wave at locations along the pressure tube were determined from the framing camera record, and the acceleration of the phased detonation wave along the pressure tube was calculated. The observed acceleration was found to be identical to the programmed acceleration. The shock wave generated in the pressure tube by the accelerating virtual piston followed the expected trajectory during the early phases of the lens operation.

The experiments with the symmetrically and asymmetrically formed accelerating pistons indicated that the shock wave generated by the asymmetric implosion departs from that of the symmetric implosion only for very long lengths of shocked gas. The difference in performance between these two modes is related to the manner in which the collapse of the pressure tube takes place. The asymmetrically collapsed pressure tube is less able to prevent the loss of boundary-layer gas, so when long lengths of shocked gas are required, a symmetric implosion is more desirable. However, for applications as a second stage in the two-stage launcher, the asymmetric implosion appears to be as effective as the symmetric implosion, since the length of gas between the piston and the projectile is never large in terms of barrel diameters.

The use of asymmetric lenses has several advantages: (1) In the explosive lens, any changes in the second-stage acceleration or terminal projectile velocities requires a different lens contour; the contour of an

—Pressure Tube

t = - 1 μsec
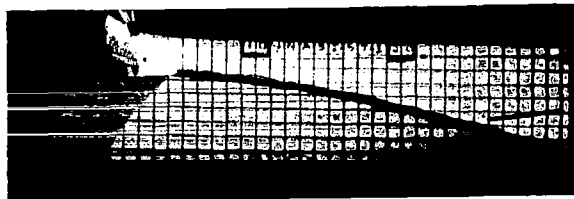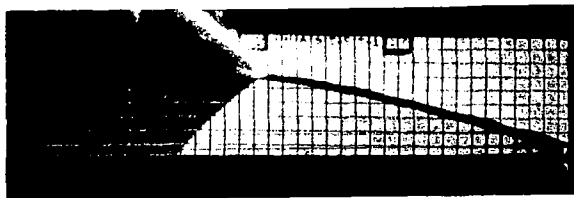
t = 20 μsec
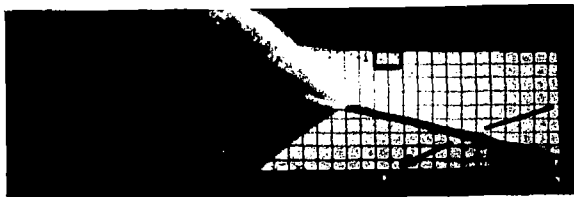
—Bridge Wire for
Determining Timing

t = 40 μsec
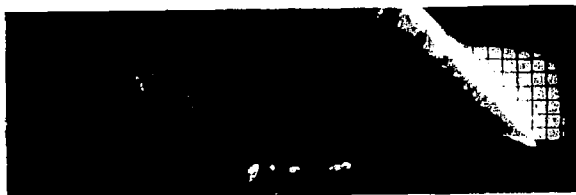
t = 60 μsec

Note: Zero time taken as
the arrival time of
the phased detonation
wave at the lens axis,
or the location of the
pressure tube.

t = 80 μsec

FIGURE 17. EXPLOSIVE LENS TO ASYMMETRICALLY COLLAPSE
THE PRESSURE TUBE

asymmetric lens can be traced on sheets of plastic or metal and cut out
rather easily, permitting designs and techniques to be evaluated rapidly.
(2) By adopting the asymmetric design, the required amount of explosive is
reduced considerably. (3) The asymmetric design permits complete optical
coverage of the lens operation, where the symmetric does not.

E. TWO-STAGE LAUNCHER PERFORMANCE

The first two-stage launcher system tested, utilized the asymmetric
implosion technique in the second stage. Initiation of the second-stage lens
was accomplished by using the response of a contact pin located at the initial
projectile position, which permits the two-stage gun to be self-timing. The
complete launcher is shown immediately before firing in Figure 18.

Because of the lack of experience with extremely high velocities,
the first launching was conducted into a range of helium at one atmosphere
and thin foil range switches were used to fire down the range radiograph
units. This first test, in which the operation of the second stage was near
ideal, resulted in a terminal projectile velocity of 12.2 km/sec. However,
the 0.17-gram lithium-magnesium projectile was partially fragmented, as
Figure 19 shows. Figure 20 illustrates in the time-distance plane the close
agreement between the observed and calculated performances of the complete
two-stage system.

This experiment was subsequently repeated, except that the range
atmosphere was reduced to 20 mm Hg of air and the range radiographs were
triggered by preset delays. The velocity of the projectile was again
12.2 km/sec, and the projectile was partially fragmented as in the first
launching. The detailed performance of the two-stage gun used in this
second experiment was identical to the performance of the one used in
the first.
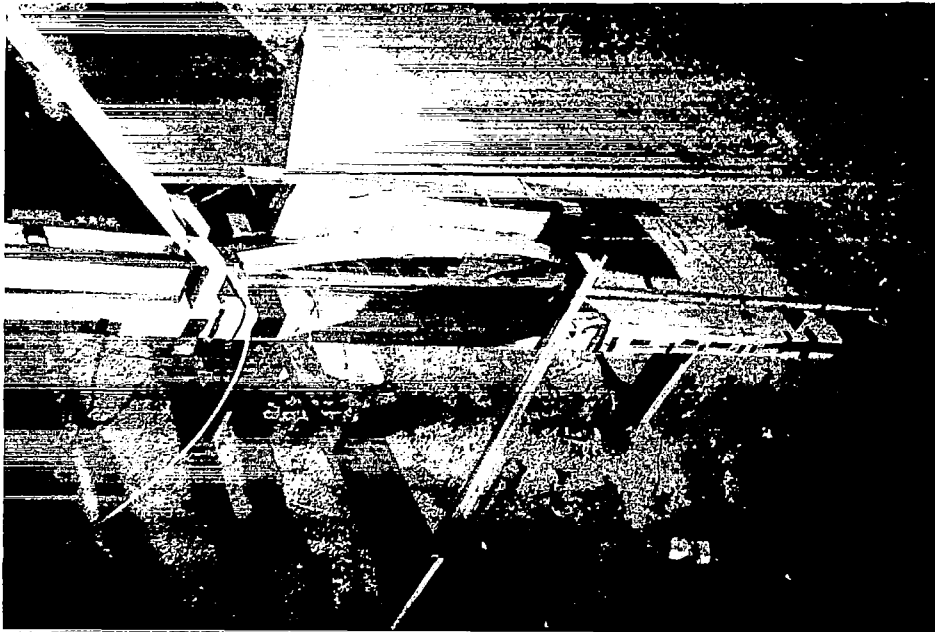
a. Two Stage Launcher Used to Accelerate a 0.17 gm Projectile to 12.2 km/sec
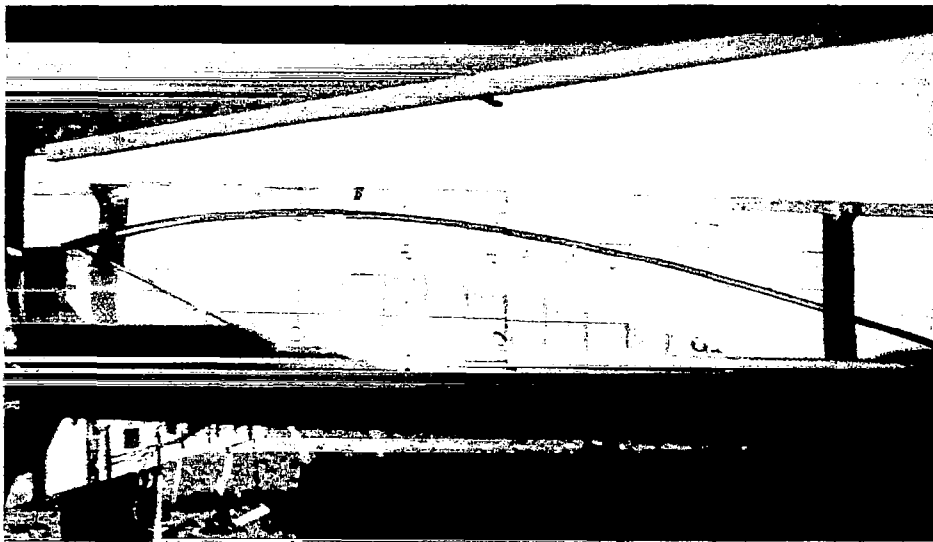
b. Asymmetric Explosive Lens Used as the Second Stage of the Two Stage System

FIGURE 18.   TWO-STAGE LAUNCHER
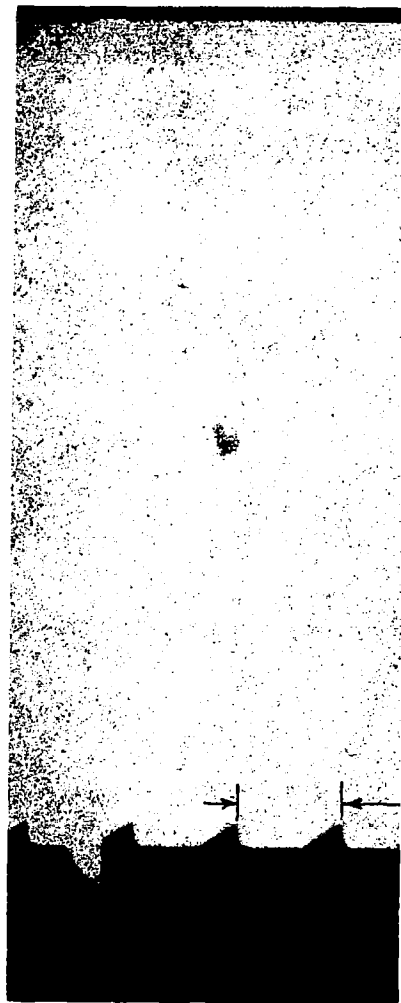
Projectile

Weight = 0.17 gm
Diameter = 0.66 cm
Length = 0.36 cm

0.5 in.

60 cm from Muzzle

FIGURE 19. RADIOGRAPH OF LITHIUM-MAGNESIUM
PROJECTILE IN FREE FLIGHT AT 12.2 km/sec
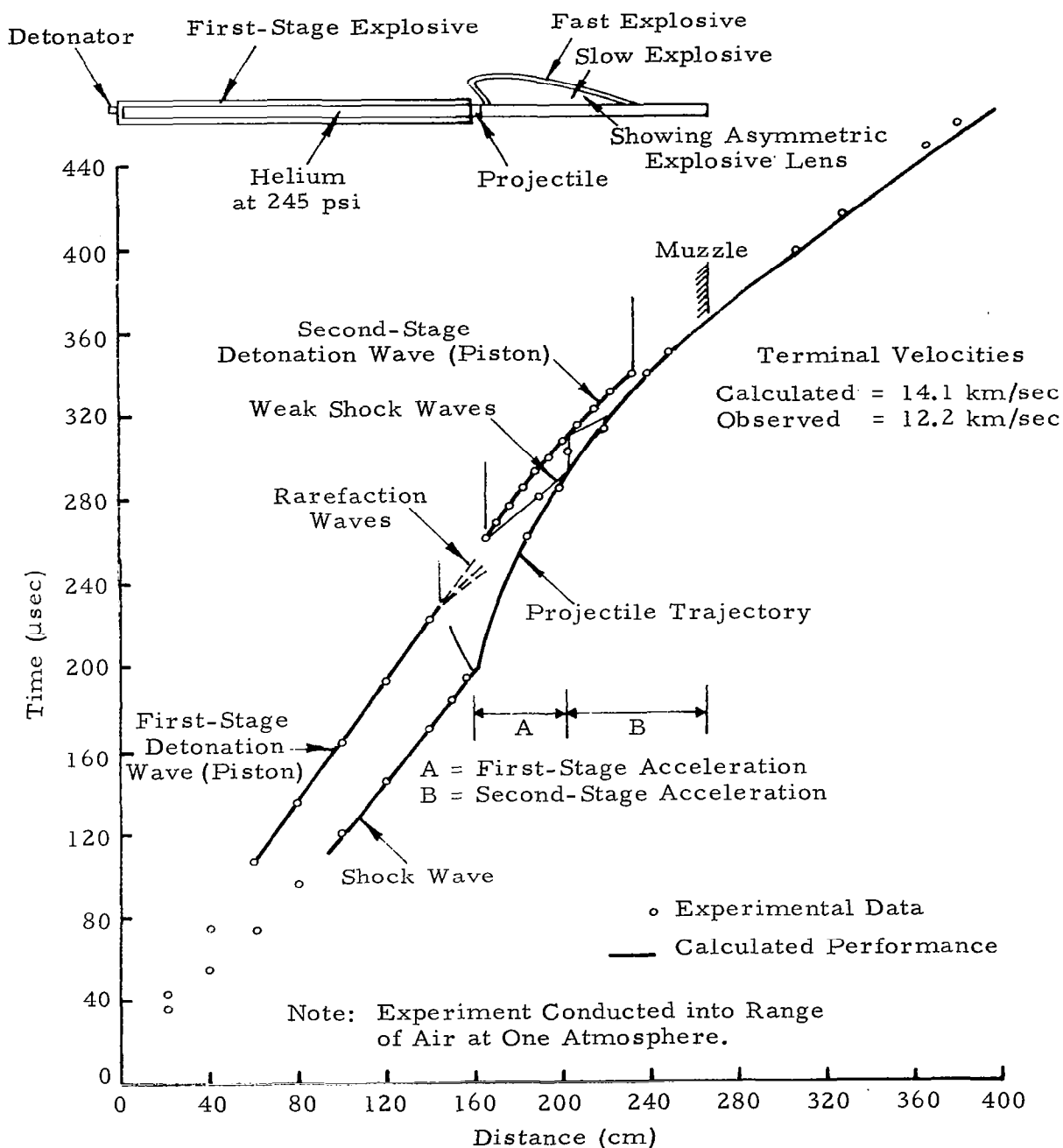
FIGURE 20.   PERFORMANCE OF A TWO-STAGE EXPLOSIVELY
DRIVEN LIGHT-GAS GUN

Since the projectiles used in the first two experiments behaved in a similar manner, in spite of the vastly different range conditions, the second-stage acceleration cycle was re-examined as a possible cause of projectile damage. It was noted that as the detonation front in the second stage accelerates from 5.5 km/sec to 12.5 km/sec, the length of the cone-shaped piston becomes nearly as large as the calculated distance between an ideal planar piston and the projectile (Figure 9). Thus, for the gasdynamic cycle chosen for this two-stage gun, the projectile is potentially in danger of becoming trapped in the cone-shaped region of the explosively formed piston. Indeed, if there is any driver gas lost through the piston during the second-stage acceleration, the projectile could be fragmented by an encounter with the cone-shaped piston. The second-stage performance calculation indicates that this encounter would occur late during the acceleration of the projectile.

Assuming that the asymmetrically formed, second-stage piston had allowed a significant leakage of driver gas, the two-stage system was retested using a full three-dimensional explosive lens as the second stage. It was hoped that the resulting symmetric, second-stage piston would be well enough formed to prevent an encounter between the piston and the projectile. This experiment was carried out into a range atmosphere of 20 mm Hg of air, and again the range radiographs were triggered by preset delays. Although the two-stage system operated as programmed, the projectile emerged fragmented at 10.0 km/sec.

The above tests have established the feasibility of launching projectiles to velocities that are unobtainable by conventional light gas guns. The observed performance of the first-stage launcher and the second-stage lens was in very good agreement with the calculated performance. The programmed base pressures on the projectile are well within previously demonstrated limits for intact projectiles. The inability to launch an intact

projectile with the present design is basically a consequence of the improper matching of the first- and second-stage characteristics. That is, the present second-stage lens design requires that the pressure of the driver gas injected by the first stage be approximately 4 kb in order to maintain a near constant base pressure on the projectile. Conversely, the 1.3-kilobar driver gas actually injected by the first stage dictates a second-stage lens with substantially lower acceleration than the acceleration used in the above tests (Figure 8). The present acceleration was chosen to expedite the fabrication, assembly, and testing of the two-stage explosively driven gun. When the pressure of the driver gas delivered to the second stage is more compatible with the acceleration of the second-stage piston, the distance between the piston and the projectile varies only a few percent during the acceleration. Therefore matching the first- and second-stage characteristics would eliminate the possibility of trapping the projectile in the implosively-formed accelerating piston.

SECTION III

IDEAL PERFORMANCE OF THE LINEAR EXPLOSIVE DRIVER

The explosive driver represents a new generation of hypervelocity test devices in which a portion of the chemical energy of an explosive is converted to the kinetic and internal energy of a gas. This process occurs in a controlled manner to produce specific energy densities in the gas which are considerably higher than those obtainable by more conventional techniques. The basic mechanism of energy conversion utilizes the pressure developed behind a detonation wave to progressively collapse a gas-containing metal tube. The implosion of the tube forms a cone-shaped piston that drives a strong shock wave into a column of gas. The velocity of the piston, and hence of the gas, is determined by the particular explosive system used. For example, the two-stage launcher employs two different types of piston motion: (1) a constant-velocity piston generated by the linear explosive driver of the first stage, and (2) the uniformly accelerated piston produced in the second stage by the explosive lens.

For completeness, a brief review of the ideal performance of the linear driver is given below. While this description assumes a constant-velocity piston, the analytical methods introduced here are generally applicable to all drivers involving the progressive implosion of a tube containing gas.

The operational concepts of the linear explosive driver are illustrated in Figure 21. A thin-walled metal cylinder serves as a pressure tube containing the driver gas. This tube is surrounded by a concentric cylinder of high explosive. After the explosive is initiated at the closed end of the tube, a detonation wave propagates in the cylinder of explosive. The high pressure behind the detonation wave accelerates the walls of the pressure tube inward toward the axis, sealing the tube and forming a cone-shaped,

Explosive

Pressure Tube   Driver Gas

Detonator

a. Time = 0, Before Initiation of the Explosive

Collapsed
Pressure Tube   Detonation Wave

Shocked Driver Gas

D

S

Shock Wave

Detonation Wave

b. Time = $\overline{t}_1$ After Initiation of the Explosive

Detonation Wave
(Ideal Piston)

$\overline{t}_1$

D   S

Ideal Shock Wave

Length of Shocked Driver Gas

$\overline{t} = \dfrac{Dt}{d}$ (Dimensionless Time)

$\overline{x} = \dfrac{x}{d}$ (Dimensionless Distance)
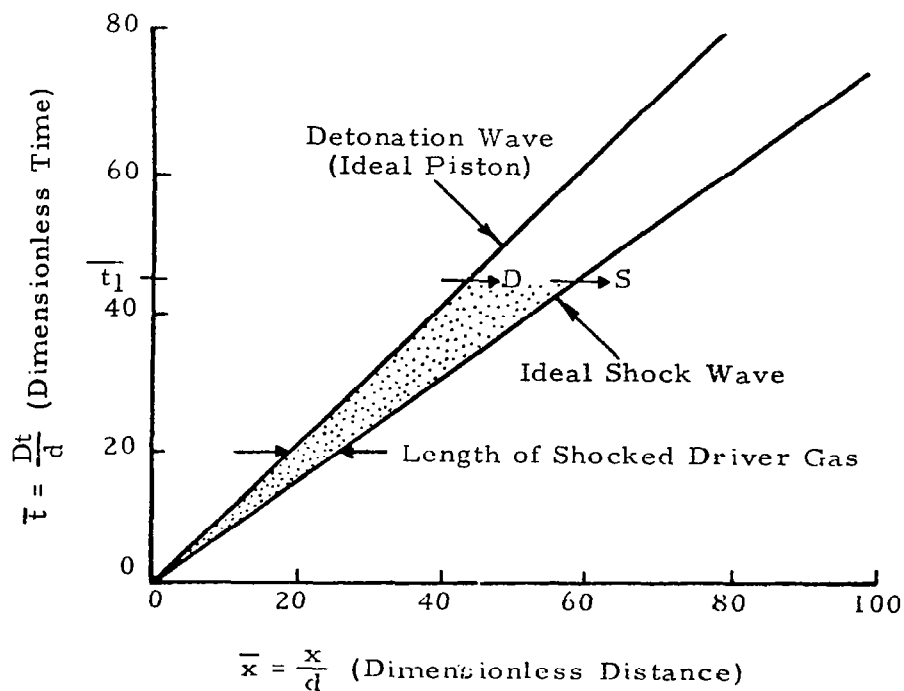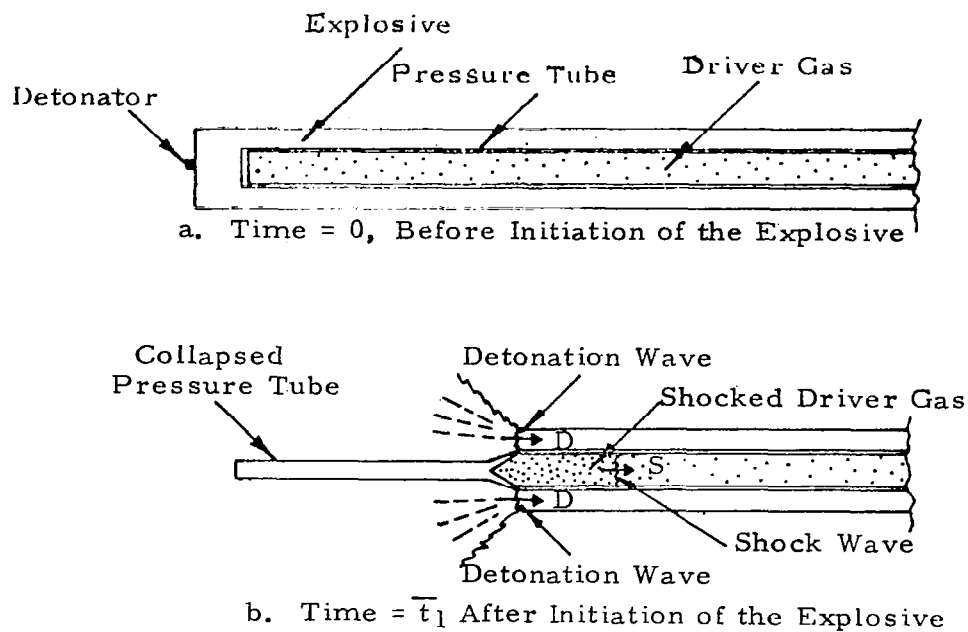
c. Position-Time History of Shock and Detonation Wave

FIGURE 21.   IDEAL OPERATION OF THE LINEAR
EXPLOSIVE DRIVER

35

piston (Figure 21b). This piston has a constant axial velocity equal to the detonation wave velocity in the explosive. The motion of this piston generates a strong shock wave in the stationary driver gas, which accelerates it to the velocity of the piston. In addition, the shock wave produces an internal energy density in the gas that is equal to its kinetic energy density.

For an ideal gas, the conservation of mass across the shock front requires the velocity of the shock wave to be $\frac{\gamma + 1}{2}$ times the velocity of the piston, where γ is the ratio of the specific heats of the gas. Figure 21c shows the ideal position-time histories of the piston and the shock wave. These trajectories are presented in the dimensionless coordinates

$$\bar{x} = \frac{x}{d} \quad \text{and} \quad \bar{t} = \frac{Dt}{d} .$$

Here x and t are the distance and time, respectively, after the shock wave begins to move ahead of the detonation wave, d is the internal diameter of the pressure tube, and D is the detonation velocity of the explosive. The use of these coordinates facilitates the comparison of drivers having pressure tubes of different dimensions or utilizing explosives with different detonation velocities. It should also be noted that in this coordinate system all slopes are normalized with respect to the detonation velocity; they become ratios of velocities of which the denominator is detonation velocity. For example, in Figure 21c the trajectory of the detonation wave has a slope of 1

$$\frac{d\bar{x}}{d\bar{t}} = \frac{1}{d} \cdot \frac{d}{D} \cdot \frac{dx}{dt} = \frac{1}{d} \cdot \frac{d}{D} \cdot D = 1.$$

Similarly, the trajectory of the ideal shock wave has a slope of $\frac{\gamma + 1}{2}$ (4/3 for $\gamma = 5/3$). Figure 21c also shows that for the ideal driver the length of shocked gas, the distance between the shock wave and piston, increases linearly with distance and is limited only by the length of the driver.

The pressure P_2 in an ideal gas behind a strong shock wave is given by the conservation of momentum as

$$P_2 = P_1 + \rho_1 \frac{\gamma + 1}{2} D^2$$

where P_1 and ρ_1 are the pressure and density of the stationary gas ahead of the shock, γ is the ratio of specific heats of the gas, and D is the velocity of the shocked gas, the detonation velocity. This relationship is indicative of how conditions in the shocked gas can be varied over a considerable range of gases (γ), initial loading densities (ρ_1), and explosives (D).

Table I lists the dynamic and thermodynamic properties produced in helium by a typical explosive driver used for accelerating projectiles.

TABLE I

PROPERTIES PRODUCED IN HELIUM BY A TYPICAL
EXPLOSIVE DRIVER

Gas Velocity . . . . 6.42 km/sec
Pressure . . . . 3.98 kb[*]
Density . . . . 0.0312 gm/cm^3[*]
Internal Energy Density . . . . 20,600 J/gm[*]
Kinetic Energy Density . . . . 20,600 J/gm
Specific Enthalpy . . . . . . 34,400 J/gm[*]
Temperature . . . . 6,600° K[*]
Sound Speed . . . . 4.78 km/sec[*]

[*]As calculated, assuming helium behaves as an
ideal gas with a ratio of specific heats (γ) of 5/3.

It is noted that for an ideal gas the magnitude of each of these properties except density is a function only of the detonation velocity of the explosive used. For this particular driver, whose explosive was nitromethane, the detonation velocity was 6.42 km/sec. The initial pressure of the helium

was 645 psi. The observed performance of this driver is shown in Figure 22. It is seen that the shock trajectory closely follows the ideal strong shock prediction.
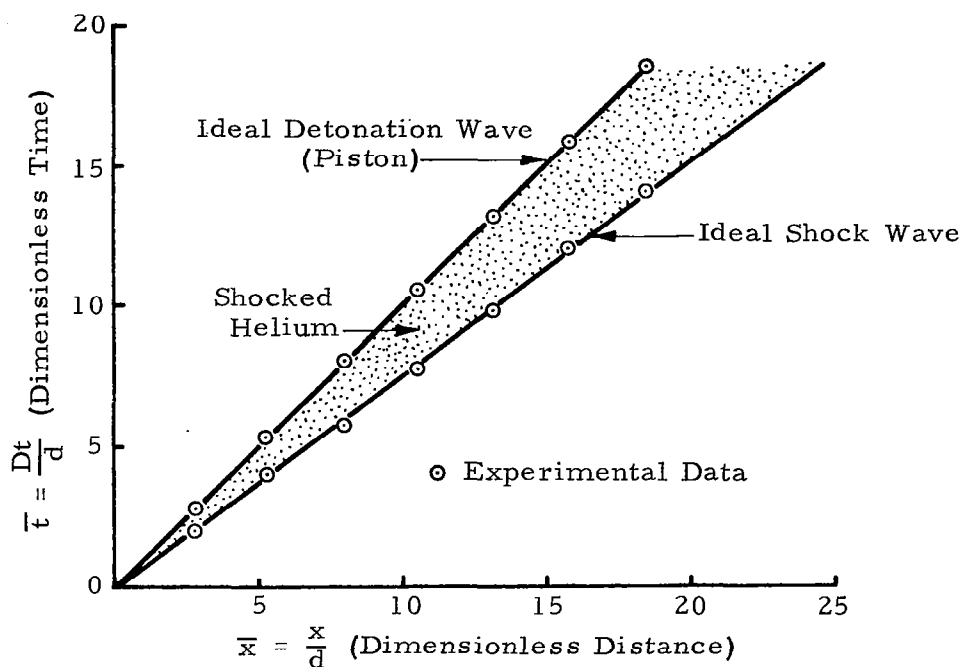
FIGURE 22. PERFORMANCE OF A 4-kilobar EXPLOSIVE DRIVER

When a linear explosive driver is used to launch projectiles, the shock wave in the driver gas reflects from either the projectile, as in an unchambered gun, or from the area change, or "breech," as in a chambered gun. The reflected shock brings the gas essentially to rest, converting its available kinetic energy to additional internal energy. This process produces a reservoir of gas having an extremely high, energy density. For example, if the thermodynamic state of the gas prior to this reflection

is given by the properties listed in Table I, the properties in the gas behind the reflected shock include those given in Table II.

TABLE II

PROPERTIES PRODUCED IN HELIUM BEHIND A REFLECTED SHOCK

Pressure	~ 20 kb
Density	~ 0.08 gm/cm^3
Temperature	$\sim 15,000^\circ$ K
Sound Speed	~ 7 km/sec

These values are estimates based on the reflection of a strong shock wave traveling in an ideal gas and being reflected from a perfect "stone wall."

SECTION IV

OBSERVED PERFORMANCE OF THE LINEAR EXPLOSIVE DRIVER

An extensive series of experiments was conducted during the past year to investigate the performance of the linear explosive driver. The primary objective of these experiments was to support the design and development of the two-stage launching system by investigating the progressive collapse of a gas-containing metal tube over a wide range of experimental parameters. The results of this study showed certain departures from the ideal driver performance described in the previous section. Considerable effort was then expended to relate the observed driver behavior to the mechanisms that control this behavior. Three phenomena were incorporated in a model of explosive-driver operation to account for observed driver performance. They are: (1) radial expansion of the pressure tube behind the shock wave, (2) the effect of boundary-layer growth behind the shock wave, and (3) formation of a metal or metal-gas jet by the collapsing pressure tube. These phenomena are interrelated through the kinetics produced by the imploding pressure tube. Their interdependence is such that changes in driver behavior resulting from certain experimental parameter changes cannot be attributed solely to one particular phenomenon. However, the ability of the model to explain, predict, and control the behavior of explosive drivers justifies the categorization of these phenomena.

A. EXPANSION OF THE PRESSURE TUBE

If the pressure in the gas behind the shock wave exceeds the dynamic yield strength of the pressure tube, the walls of the tube will begin to expand radially. For relatively short lengths of shocked gas, the expansion is almost negligible since further expansion is prevented by the detonation wave that closely follows. For longer lengths of shocked gas, however, the tube

expansion becomes extremely important. It allows the shocked gas to expand, which reduces the pressure in the gas and decreases the velocity of the shock wave. The shock trajectories shown in Figure 23 demonstrate this effect. Diluted nitromethane with a detonation velocity of approximately
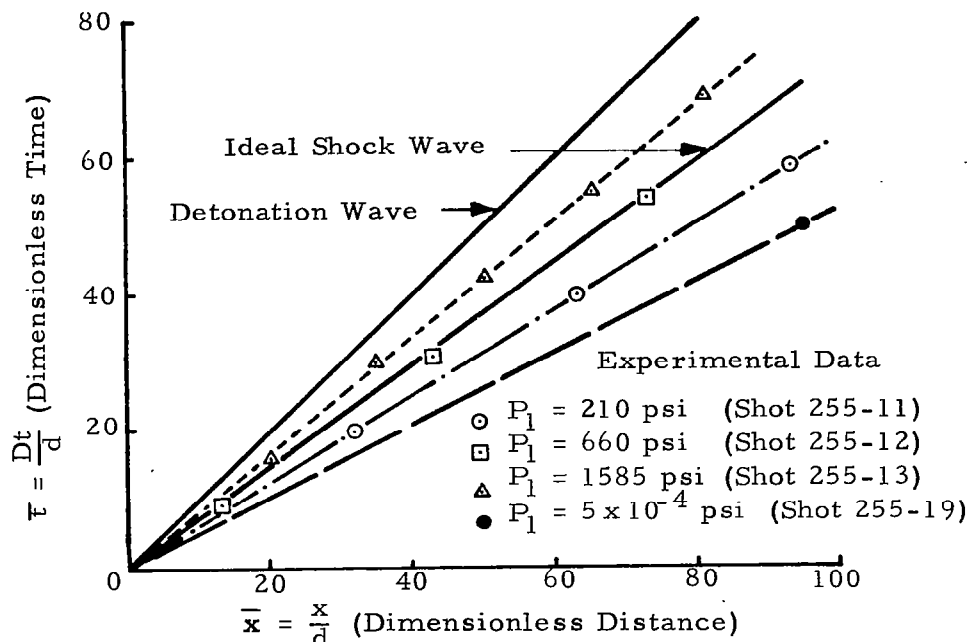
FIGURE 23. COMPARISON OF SHOCK TRAJECTORIES PRODUCED BY THE PROGRESSIVE COLLAPSE OF A 0.316-inch OUTER DIAMETER TIMES 0.258-inch INNER DIAMETER STEEL TUBE CONTAINING HELIUM AT VARIOUS INITIAL PRESSURES

5.5 km/sec was used for these experiments to progressively collapse a 0.316-inch external diameter by 0.258-inch internal diameter steel tube. It is seen that as the pressure increases the shock velocity decreases. The observed shock velocities correspond to pressures of 1.3, 3.4, and 6.0 kb in the shocked helium for the initial pressures of 210, 660, and 1585 psi, respectively. It is also noted that for the initial loading pressures of 5×10^{-4} psi and 210 psi, the observed shock velocities

are considerably higher than ideal predictions. This is attributed to the formation of a metal or metal-gas jet discussed in a following section.

In addition to causing shock attenuation, tube expansion will eventually lead to rupture of the pressure tube. Figure 24 shows a radiograph of an expanding 1015-steel pressure tube. Longitudinal fractures resulting from the expansion can be seen between the shock and detonation waves. The initial pressure behind the shock wave for this experiment was approximately 10 kb, which had decayed to 5 kb at the time of this radiograph.

For reasonably low gas pressures, the thickness of the pressure tube walls can be increased to reduce radial expansion. However, at higher pressures the wall thickness becomes prohibitively large and increasingly more difficult to collapse. The trajectories shown in Figure 25 illustrate the effect of increasing the wall thickness δ of the pressure tube from the 0.028 inches used in the experiments described in Figure 23 to 0.067 inches.
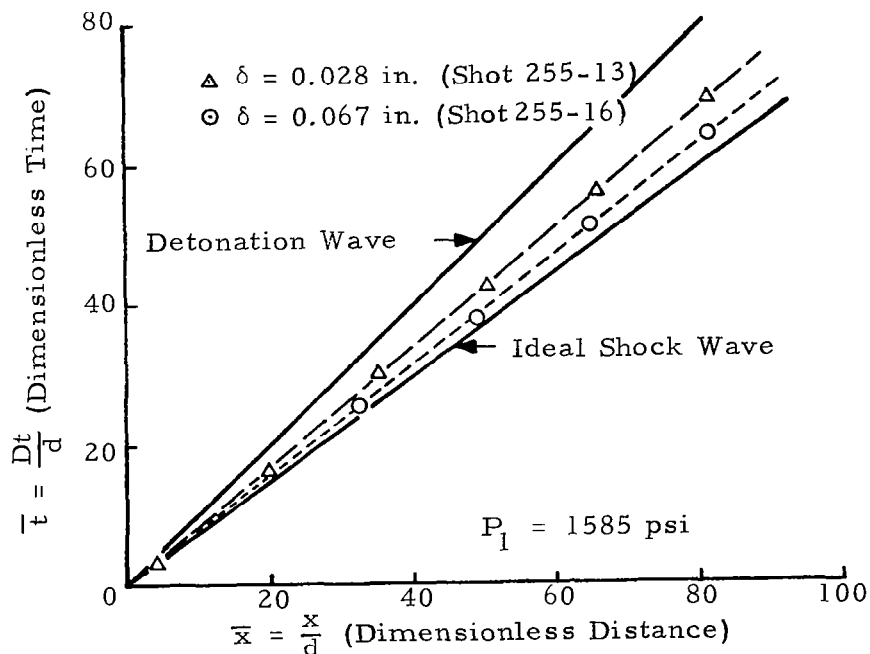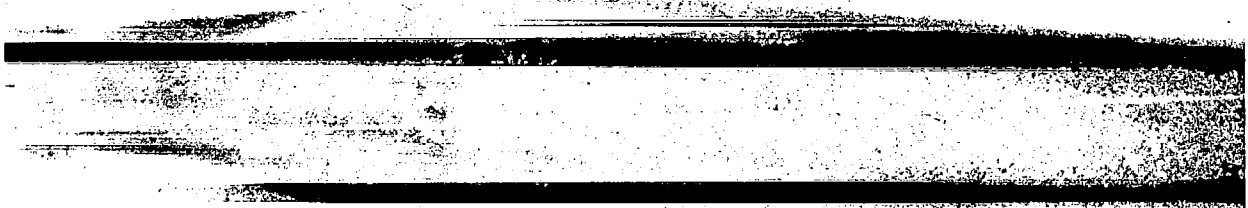

FIGURE 25. COMPARISON OF SHOCK TRAJECTORIES PRODUCED BY THE PROGRESSIVE COLLAPSE OF STEEL TUBES, 0.258-inch INSIDE DIAMETER, HAVING DIFFERENT WALL THICKNESSES

9/16-inch Outer Diameter x 0.035-inch Wall

a. Before Initiation of Explosive

Detonation Wave

b. 112 μsec After Initiation of Explosive

FIGURE 24. RADIOGRAPH OF PRESSURE TUBE IN AN
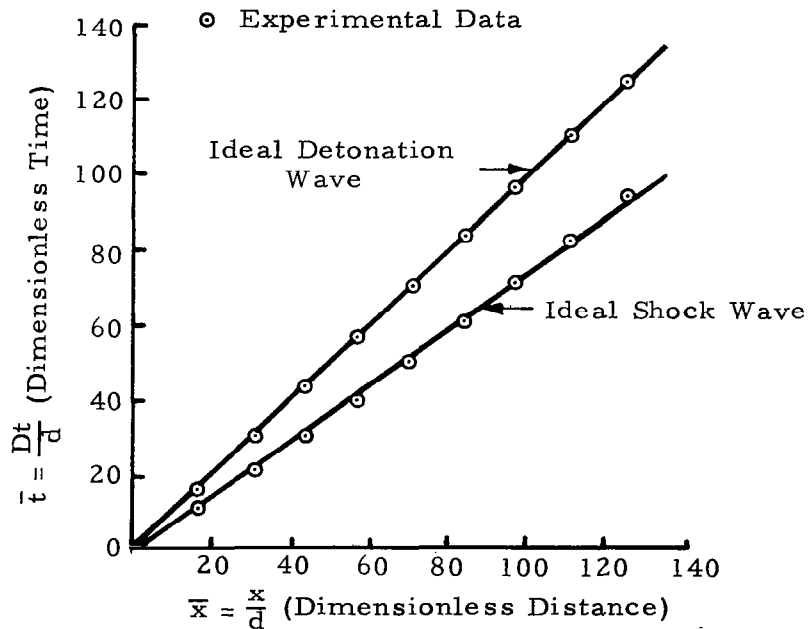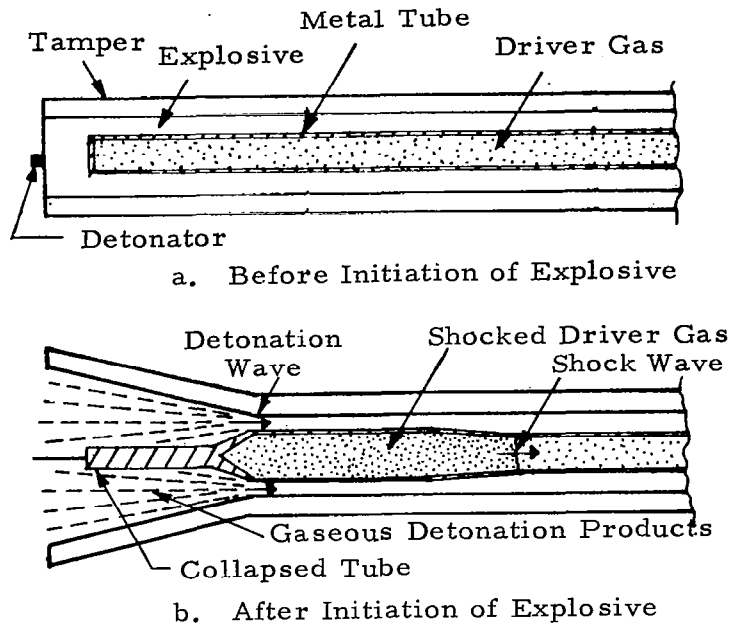UNTAMPED EXPLOSIVE DRIVER

It is seen that the use of the tube with thicker walls causes the shock velocity to increase. Since the pressure behind the shock wave for each of these experiments exceeded the dynamic yield strength of the metal tube, the additional mass of the thicker tube merely reduced the rate at which the tube expanded.

A more desirable method of limiting pressure tube expansion is to use a thick-walled pressure vessel to surround the explosive driver. This vessel is called a "tamper." The tamper is chosen to have such high yield properties that it will not yield under the pressure developed behind the shock wave. As a result, the pressure tube will expand a small amount until an equilibrium position is reached where the pressure in the explosive between the pressure tube and tamper is approximately equal to the pressure in the shocked gas. This method is illustrated in Figure 26.

The use of a tamper around the explosive driver is most important if longer lengths of shocked gas are desired. The shock trajectory given in Figure 26b shows the length of 2-kilobar shocked gas that has been obtained using a tamped driver. The internal diameter of the pressure tube used for this driver was one and a half inches. Another effect of the tamper is to delay radial expansion of the detonation products. This allows the use of thinner explosive layers for the implosion process. Even if the shocked gas pressure exceeds the dynamic yield strength of the tamper, it can be used to delay pressure tube expansion at least until the arrival of the detonation wave.

B. GROWTH OF BOUNDARY LAYER IN A LINEAR EXPLOSIVE DRIVER

Since the use of a tamper around the explosive driver minimizes the effect of pressure tube expansion, it would appear that the length of shocked gas could be made arbitrarily long. However, experimental

Tamper Explosive Metal Tube Driver Gas

Detonator

a. Before Initiation of Explosive

Detonation Wave Shocked Driver Gas Shock Wave

Gaseous Detonation Products

Collapsed Tube

b. After Initiation of Explosive

◉ Experimental Data

Ideal Detonation Wave

Ideal Shock Wave

$\bar{t} = \dfrac{Dt}{d}$ (Dimensionless Time)

$\bar{x} = \dfrac{x}{d}$ (Dimensionless Distance)

c. Wave Trajectories of a 2-kilobar Tamped Driver

FIGURE 26. IDEAL AND OBSERVED PERFORMANCE OF A TAMPED EXPLOSIVE DRIVER

45

attempts to do this revealed a new driver behavior. Figure 27 shows the wave trajectories observed for a very long (12.5 ft) tamped driver. The
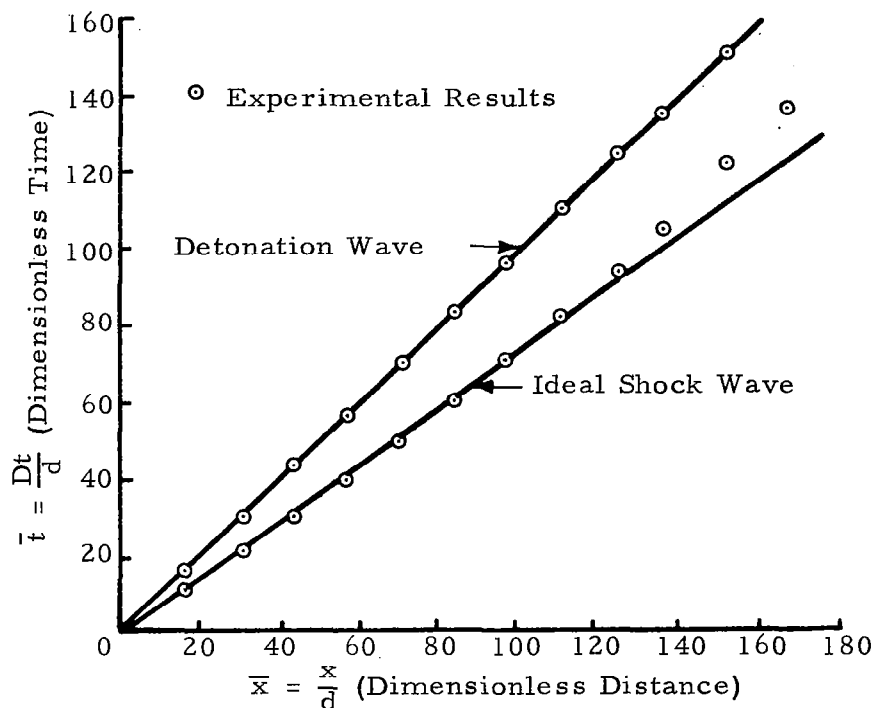

FIGURE 27. PERFORMANCE OF A LONG, TAMPED
EXPLOSIVE DRIVER

shock wave was found to have a constant velocity close to that predicted by the ideal model for approximately half of its travel in the pressure tube. At this point the shock velocity gradually decreased to a velocity that was very nearly equal to the detonation velocity. Consequently, the length of shocked gas increases uniformly at first, but eventually reaches a maximum value.

The recovery of a completely intact collapsed pressure tube provided vital insight to the driver performance described above. Inspection

of this tube showed that it was not uniformly collapsed along its axis of symmetry. Measurements showed complete closure for approximately 1/5 of the original tube length, then the internal diameter gradually began to increase until it reached a constant value that was about one-half of what it was prior to collapse. While the axial location of the tube opening did not coincide with the observed shock curvature, these locations could be linked quite successfully by a sound wave in the moving gas (u + a rarefaction wave) originating at the tube opening.

The growth of a thin boundary layer behind the shock wave was postulated as the cause of the incomplete closure of the collapsed pressure tube. As the detonation wave propagates in the explosive surrounding the tube, the walls of the tube are accelerated radially inward along with that portion of the boundary layer gas having an axial velocity less than that of the detonation wave. Since the gas in the boundary layer receives little additional axial acceleration from the implosion, it is left behind the detonation wave and trapped by the collapsing tube. This loss of gas causes downstream-running rarefaction waves which reduce the pressure and the velocity of the shocked gas and decreases the shock velocity. This loss continues until the mass flow through the shock wave equals the mass flow trapped by the collapsing liner. At this point, the shock velocity becomes equal to the velocity of the piston, the detonation velocity, and the length of shocked gas reaches a fixed, steady-state value. The trajectories shown in Figure 28 illustrate the wave system required to produce the driver performance given above in Figure 27. Pressure-distance profiles in the shocked gas are also given in Figure 28 to show one of the effects of the downstream-running rarefactions.

A semi-empirical analysis was performed using turbulent boundary-layer theory to relate the steady-state length of shocked gas ℓ_{ss} to the Reynolds number of the steady-state gas flow

$$\frac{\ell_{ss}}{d} = KRe_d^{1/4}$$

where d is the initial internal diameter of the pressure tube, Re_d is the
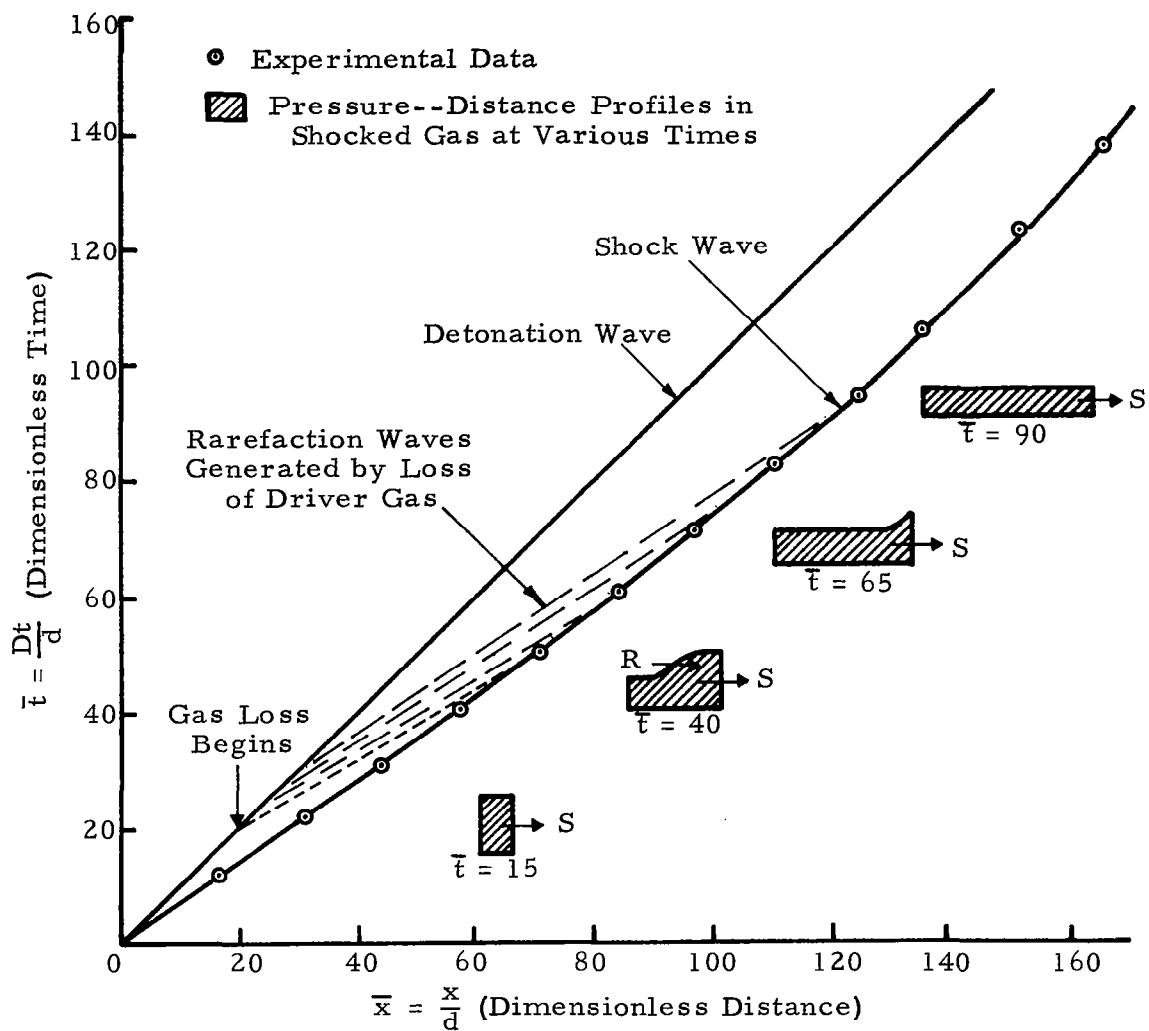
FIGURE 28. PERFORMANCE OF A LONG, TAMPED EXPLOSIVE DRIVER
SHOWING EFFECTS OF LOSING BOUNDARY-LAYER GAS IN
COLLAPSE PROCESS

Reynolds number based on tube diameter, and K is an experimentally determined constant. This relation appears to be valid for the experimental data obtained thus far. A typical length of shocked gas (in the kilobar range) for a nitromethane driver is in the neighborhood of 25 to 30 diameters.

The shock-wave attenuation produced by the entrapment of boundary-layer gas in explosive drivers is similar to that associated with conventional shock tubes. In conventionally-driven shock tubes, the test time and the length of shocked test gas are limited by the boundary-layer gas that flows out of the test gas region and into the driver gas. This flow attenuates the shock wave while accelerating the contact surface separating the test gas and driver gas. Attempts have been made to correlate observed shock-wave trajectories with predictions based on Mirels' analytical investigations of shock-tube test-time limitations (Reference 3). In Mirels' analysis, (Reference 4), the communication time between the shock wave and the contact surface--the piston, in the case of the explosive driver--was not included. An existing one-dimensional computer program has been modified to incorporate this time dependence into Mirels' assumptions. The continuous communication process was treated in finite time steps involving first a delay for the boundary layer to build up at a fixed position, and then a second interval for rarefactions to overtake the shock wave. The shock trajectories calculated in this manner were in excellent agreement with the observed trajectories.

Because of the boundary-layer growth, the gasdynamic conditions in the gas were not uniform. However, approximate pressure, velocity, and density distribution within the gas can be determined by a calculative method in which the gas loss is adjusted to produce a shock trajectory identical to what is experimentally observed. Figure 29 shows the observed performance of a long tamped driver of the same diameter as the one used in the first stage of the two-stage launcher. Indicated in this figure is the location of the chambrage plane of the first-stage driver and the length of shocked driver gas (30 cm) when the shock first reaches this plane. The operation of the driver was simulated in a computer calculation in which a fictitious piston was used
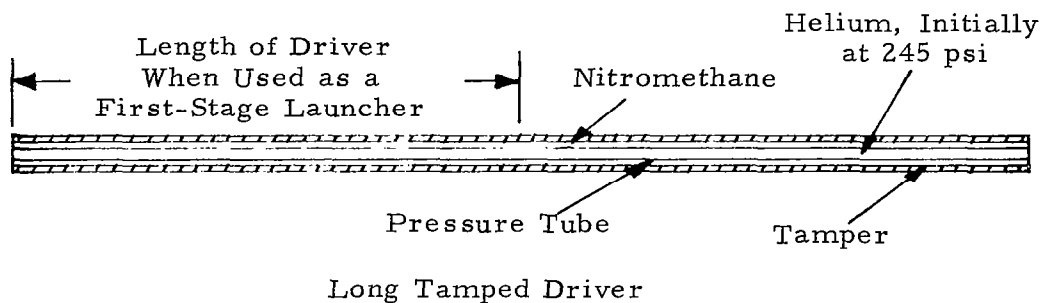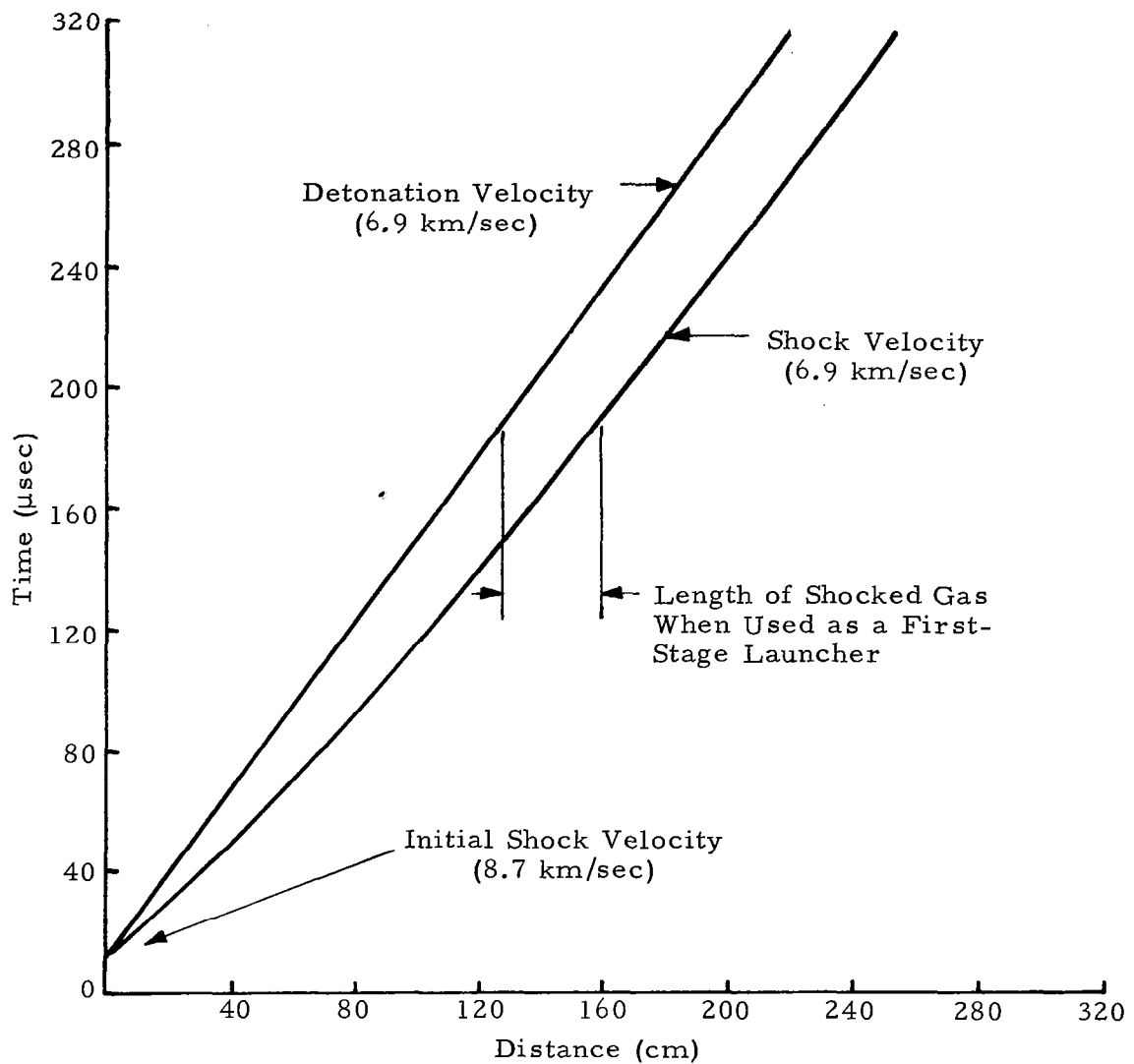
FIGURE 29. WAVE TRAJECTORIES FOR A LONG DRIVER

to generate the downstream-running rarefaction waves caused by the loss of the driver gas. Figure 30 shows the model used to simulate the observed driver performance given previously in Figure 29. The shock trajectory calculated by this model agrees closely with the observed trajectory. On this basis the calculated gasdynamic conditions behind the shock were accepted as good approximations of the actual conditions. The gas conditions calculated in this manner were used to compute the performance of the first-stage launcher. The results of this calculation were given in Section II (Figure 4).

C. JETTING PHENOMENA IN A LINEAR EXPLOSIVE DRIVER

The experimental parameters of an explosive driver can be selected to generate a wide range of driver-gas properties. Certain combinations of these parameters produce initial shock velocities that are considerably higher than those predicted by the idealized model of driver performance. For example, the experiments illustrated in Figure 23 showed that by reducing the initial gas pressure the observed shock velocities approached a value approximately twice that predicted by the ideal model. Since the implosive collapse of tubes has often been used to produce high-velocity metal jets, this velocity overshoot is attributed to the formation of a jet of tube material. An experiment was performed to determine: (1) if the observed shock velocity was a good indication of the presence or absence of jetting, and (2) whether mixing occurred between the jet-gas interface. The driver selected for this experiment was known to have a shock velocity considerably higher than the ideal predictions. A 50-centimeter length of Plexiglas tubing was used to extend the pressure tube to facilitate radiographic diagnostics. A low-voltage, high-intensity pulsed X-ray system was used to observe the Plexiglas section after the shock wave had entered the Plexiglas extension. The results of the experiment are shown in Figure 31. The radiograph taken at 60 μsec shows the existence of a very high density metal jet (Figure 31b). In addition, the observed shock trajectory indicates severe mixing of the jet with the shocked gas.
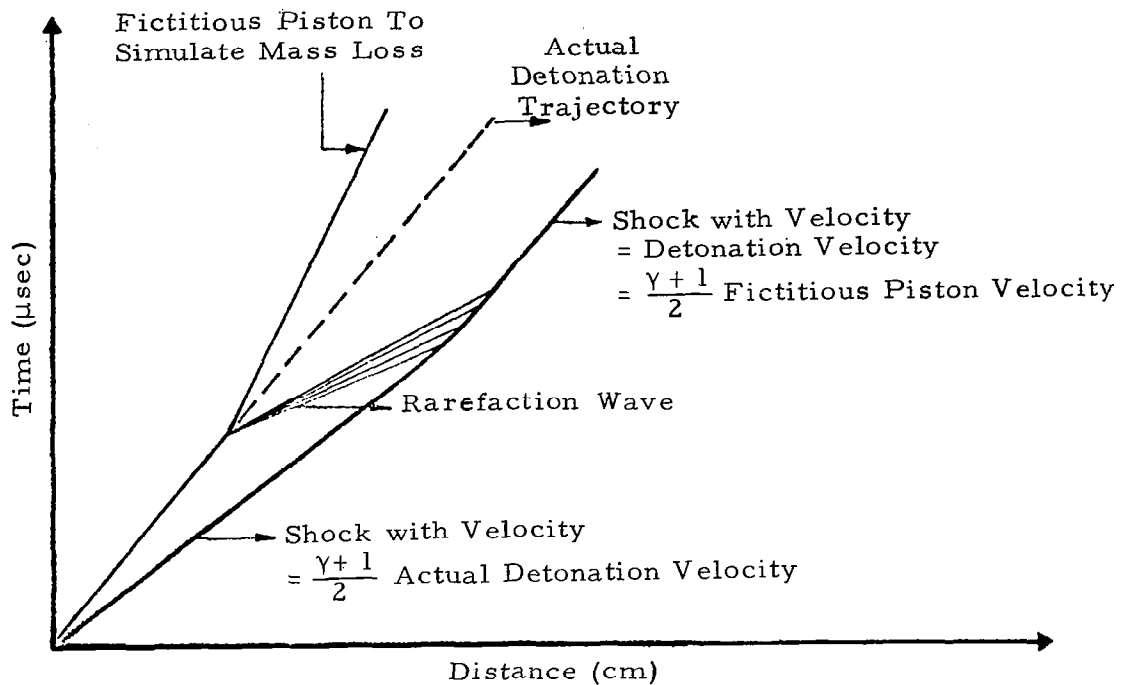
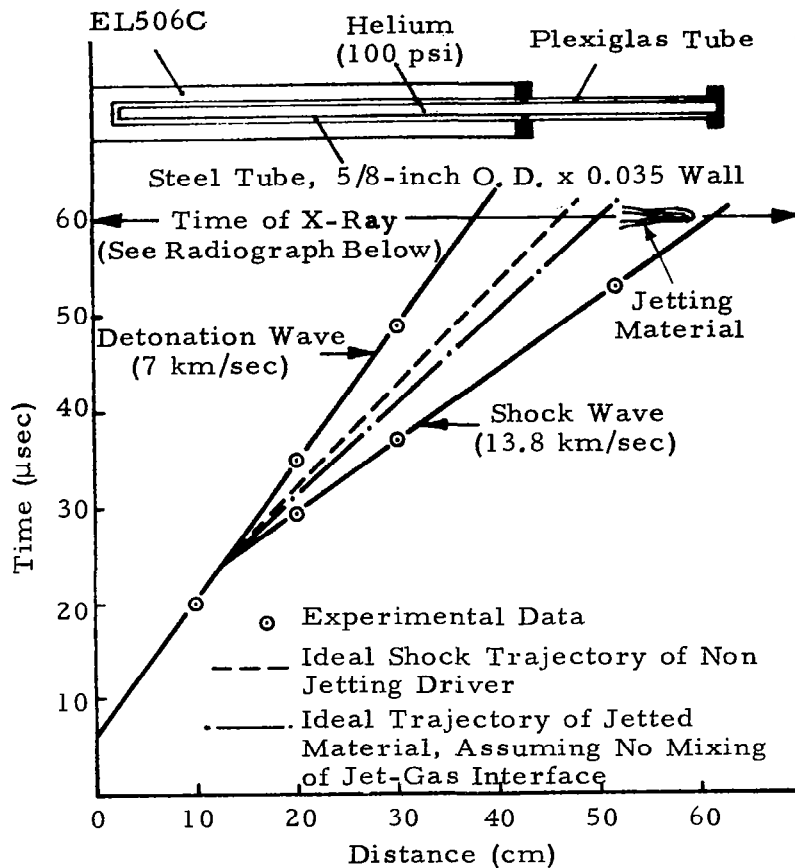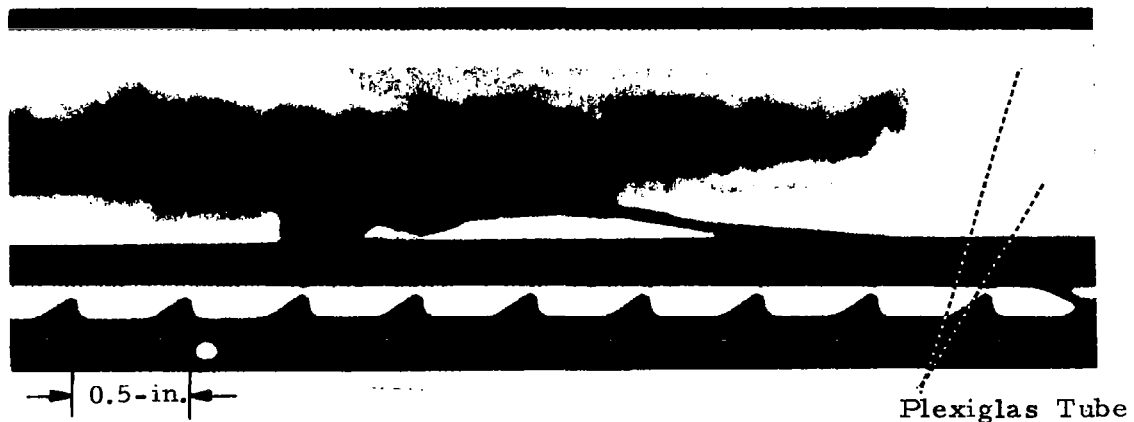a. Model Used to Simulate Observed Driver Performance
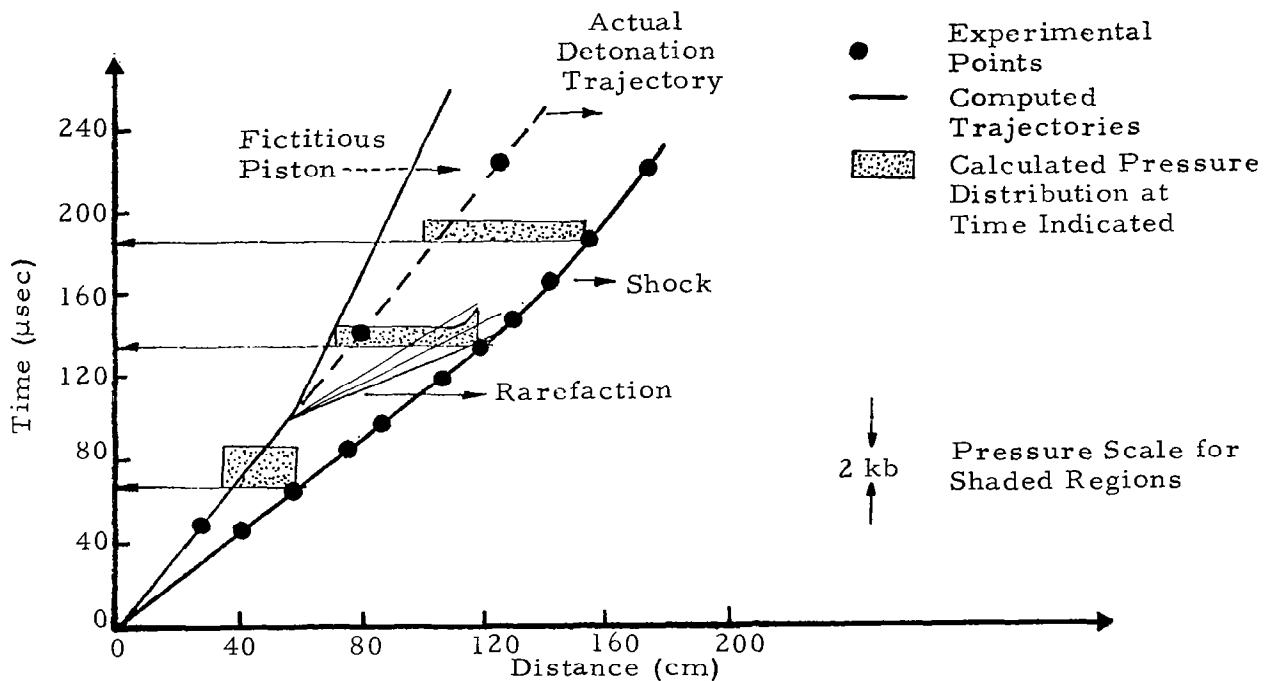
b. Observed Performance Compared with Calculated Performance Using the Model Shown in a

FIGURE 30. MODEL TO SIMULATE OBSERVED DRIVER PERFORMANCE

a. Shock Trajectory Generated by a Jetting Driver

b. Radiograph Showing Jetting Material Well Mixed
with Driver Gas 60 μsec After Initiation

FIGURE 31.   PERFORMANCE CHARÀCTERISTICS OF A
JETTING DRIVER (Shot 255-26)

Figure 32 shows the results of a similar experiment using the first-stage driver of the two-stage launching system. The radiograph given in Figure 32b showed no evidence of jet material. It is noted that the performance of the first-stage driver is dominated by boundary-layer growth. However, the later deceleration of the shock was a result of the radial expansion of the Plexiglas extension.

While not strictly applicable, the classical description of jet formation by flat plates has been used to analyze the implosive collapse of cylindrical tubes. This analysis was performed under a separate program,[*] but is summarized here for completeness. For this analysis, the colliding materials, whether flat plates or the wall of a cylindrical tube, will be referred to as liners. The mechanism of jet formation in the collision of two flat plates, as proposed by Birkhoff, et al (References 5 and 6), is shown in Figure 33.
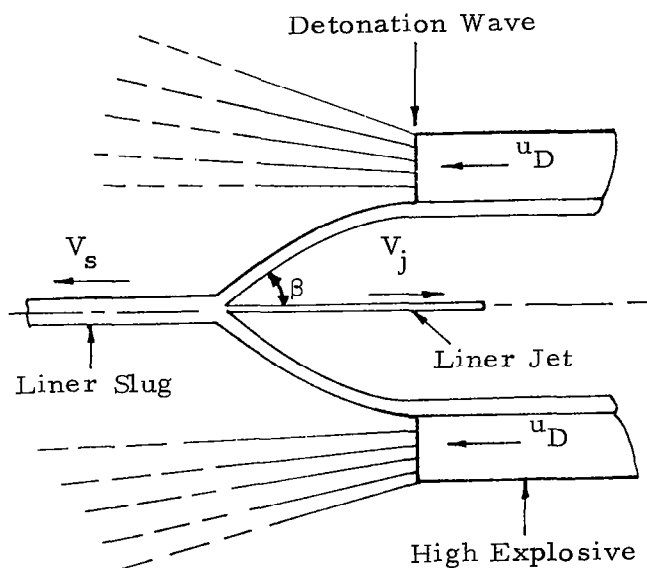
Note: All velocities are measured
relative to the detonation wave.

FIGURE 33.   FORMATION OF A METAL JET FROM THE
COLLISION OF TWO PLATES
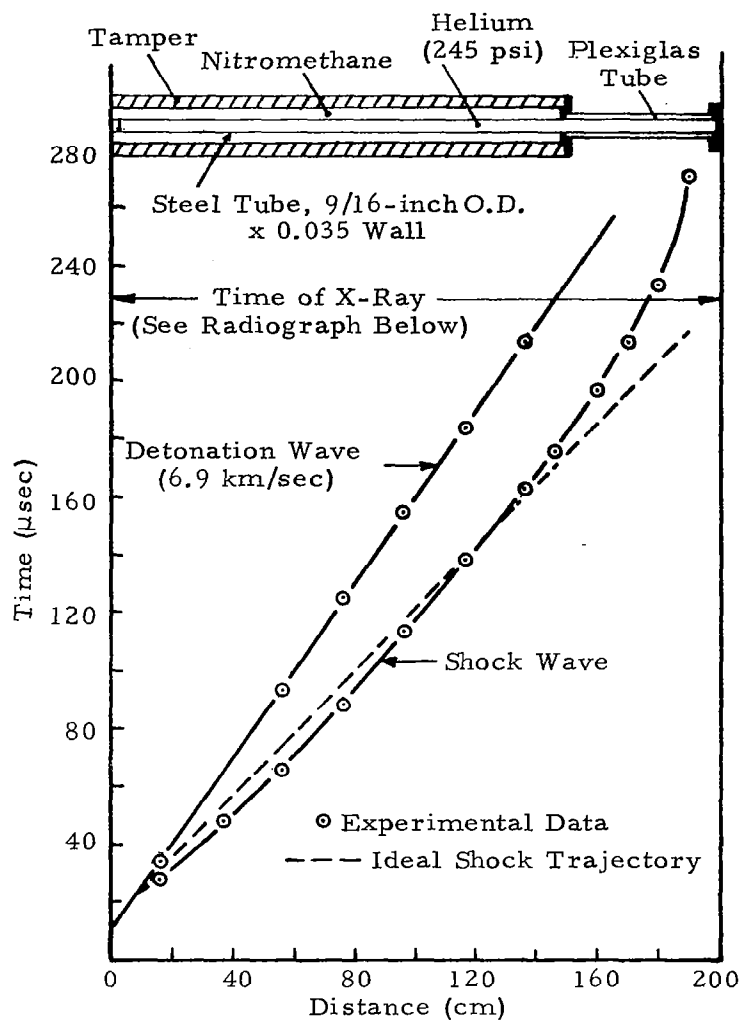
a. Shock Trajectory Generated by First-Stage Driver

b. Radiograph of Shocked Driver Gas 222 μsec After Initiation

FIGURE 32. RESULTS OF AN EXPERIMENT TO INVESTIGATE THE
EXISTENCE OF JETTING IN THE FIRST-STAGE DRIVER
(Shot 255-28)

In their analysis of the jet formation, the flow in the plates is treated as incompressible and inviscid, and as subsonic relative to the velocity of the detonation wave. Mild collisions are not treated, because the pressures generated are assumed to be sufficiently large so that material strength can be neglected. By applying Bernoulli's equation to the streamlines in the colliding plates, they show that the jet and the slug velocities, V_j and V_s respectively, equal the incident flow velocity u_D. Conservation of momentum in the axial direction yields the following equations for mass flow in the jet, m_j, and in the slug, m_s

$$\frac{m_j}{m} = \sin^2 (\beta/2) \qquad \frac{m_s}{m} = \cos^2 (\beta/2)$$

where β is the collapse angle of the plates and m is the total mass flow entering the system.

In collapsing tubes the flow in the liner will normally be supersonic rather than subsonic. Figure 34a shows a cylindrical tube collapse where a single oblique shock is sufficient to turn the flow to the axial direction. For a given supersonic flow velocity a maximum turning angle (Φ_m) will exist, as in supersonic gas flow past a wedge. If this turning angle is greater than the collapse angle at the inner surface of the liner, it is possible to satisfy the axial momentum equation without producing a jet through the formation of an attached oblique shock. That is, a liner jet will not be formed if the collapse angle of the inner surface is less than the maximum turning angle determined for the particular liner material by the flow Mach number where the Mach number is approximately equal to the ratio of detonation velocity to the local liner sound speed. Thus in order to minimize jetting it is desirable to operate with high Mach numbers in order to permit large turning angles. Also, the geometry of the liner and explosive system should be chosen so as to produce small collapse angles.

a. $\beta_s < \Phi_m$ All Liner

b. $\beta_s > \Phi_m$ Inner Portion; $\beta_s < \Phi_m$ Outer Portion
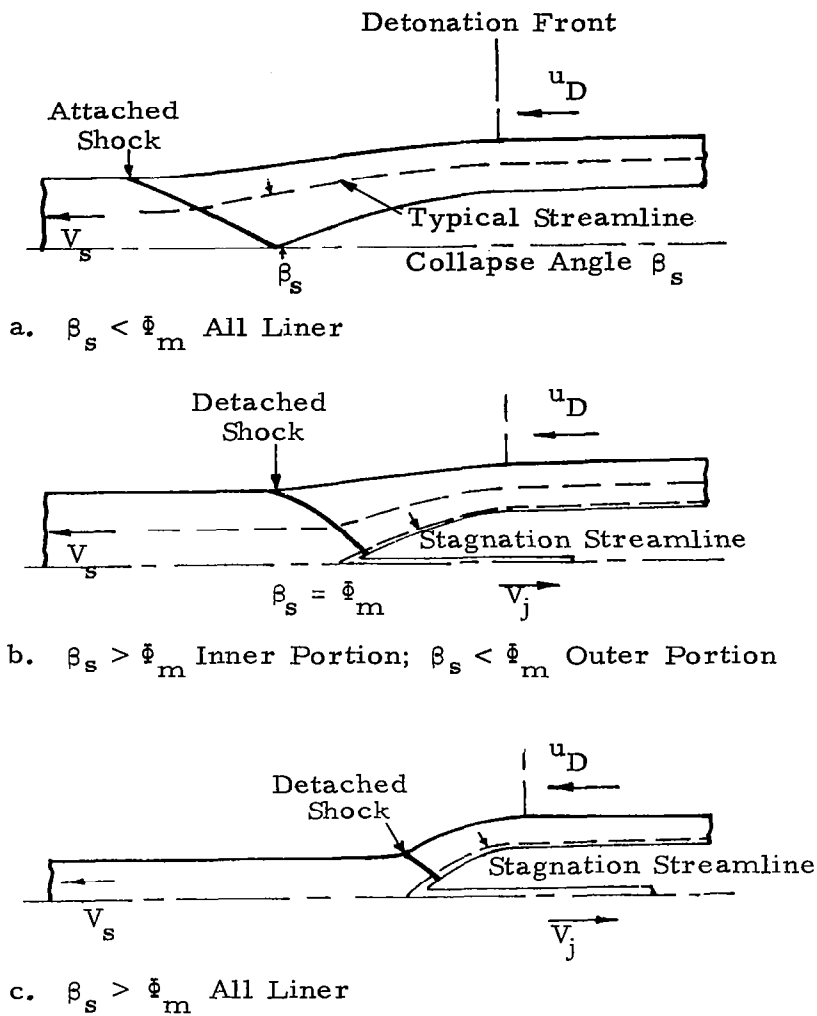
c. $\beta_s > \Phi_m$ All Liner

FIGURE 34. IMPLOSIVE COLLAPSE OF A CYLINDRICAL LINER
SHOWING JET FORMATION

If the collapse angle of the inner surface is greater than the critical turning angle, then the formation of detached shocks may be postulated. In Figure 34b two streamlines are shown: (1) the stagnation streamline that divides the material that flows into the jet from that flowing into the slug, and (2) the streamline that divides the liner material with a collapse angle greater than the maximum turning angle from that with a lesser angle. In Figure 34c the collapse angle of the outer surface is greater than the maximum turning angle of the flow, so the second streamline is not present. In both cases the detached shock is postulated to form ahead of the collapse point. Since increasing the Mach number of the liner reduces jetting, for supersonic flow, and since it is believed that the maximum jetting occurs in subsonic flow, it is desirable to operate at a high Mach number in order to minimize jetting.

From the above discussion of liner jetting, certain requirements emerge for suppressing or minimizing jetting. In particular, small collapse angles and supersonic flow conditions are required. In addition, if it is accepted that the mass in the jet is proportional to the total mass of the liner as given in the subsonic classical jetting analysis, the use of thin liners will also minimize the effect of the jet on the internal gas.

Some of the parameters that affect the collapse angle of the liner are the internal gas pressure; the inner radius, thickness, and material properties of the liner; the thickness, detonation velocity, and energy density of the explosive; and the boundary condition at the outer surface of the explosive (tamped or untamped). To evaluate the effects of these parameters, Physics International's computer programs can be used to select the particular combination of parameters to produce the desired gas conditions. Depending on the application, jetting could be suppressed or enhanced.

The above discussion of jetting assumed no boundary layer was present during the jet formation process. When we take the growth of the boundary layer into account it becomes more complex; this process is shown in Figure 35

a. No Boundary Layer, $m_j = m_L$

b. Small Boundary Layer, $m_j = m_L + m_{BL}$

c. No Tube Jet, $m_j = m_{BL}$
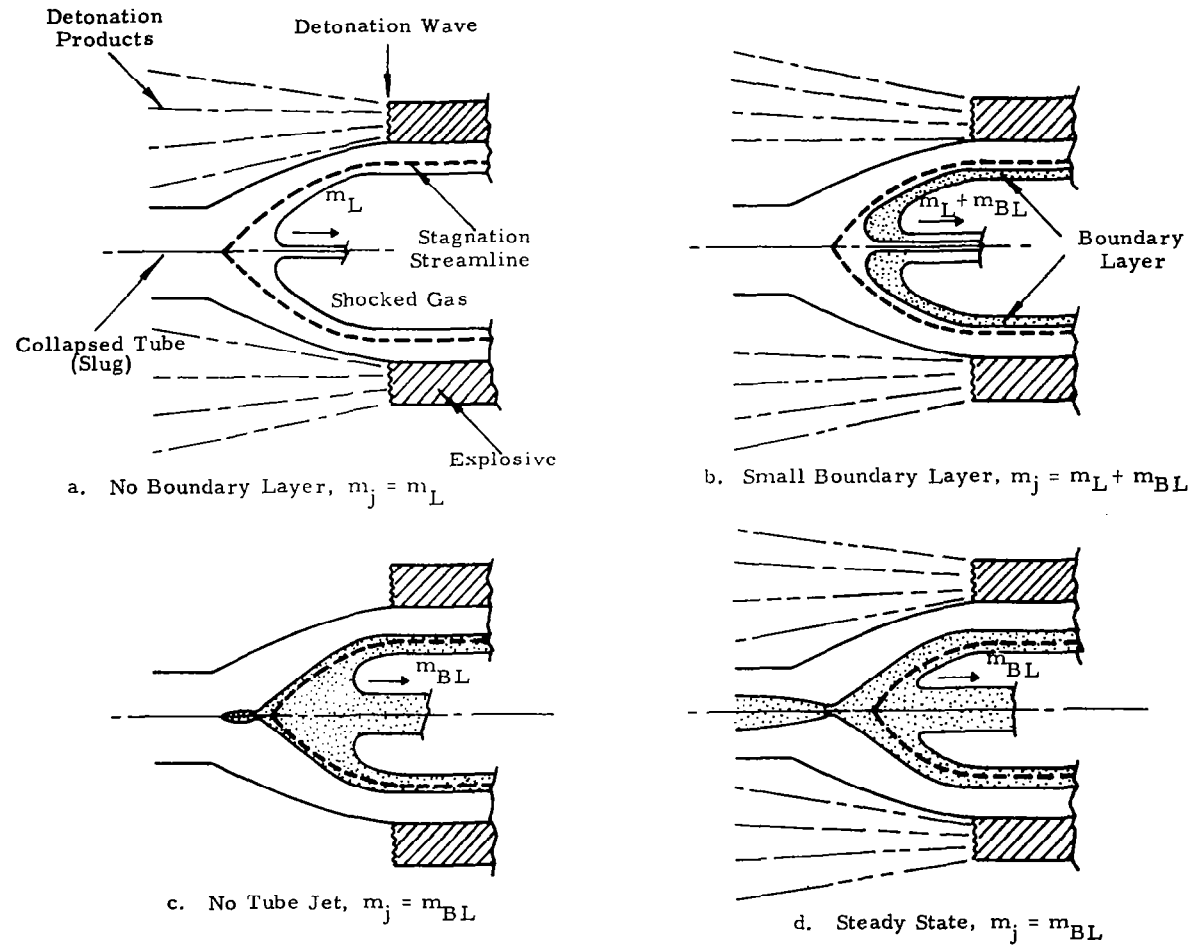
d. Steady State, $m_j = m_{BL}$

FIGURE 35. EFFECT OF BOUNDARY LAYER GROWTH (BL) ON THE COLLAPSE
OF A CYLINDRICAL LINER (L)

for four characteristic times where the reference frame is moving at detonation velocity. At early times, as in Figure 35a, the boundary-layer thickness is negligible and a mass of liner jet m_j is flowing into the shocked gas at a velocity nearly equal to the detonation velocity. A dividing streamline is shown separating the mass that flows into the jet from that flowing into the slug. Here the slug is the liner material to the left of the stagnation point. As the thickness of the boundary layer increases, the dividing streamline moves toward the inner surface of the liner as shown in Figure 35b. The jet is now composed of both liner material and boundary-layer gases. As the thickness of the boundary layer continues to increase, the dividing streamline moves past the inner surface of the liner and into the boundary layer, as shown in Figure 35c. At this time all of the liner material along with a part of the gas in the boundary layer is going into the slug, and the jet is then composed solely of the remaining portion of the boundary layer. As the boundary layer continues to grow, more gas will be lost and the gas shock continually weakened until at some time a steady state will be reached. At this time the mass of gas entering through the gas shock just equals that part of the boundary layer which is lost inside the slug. This "steady state" is pictured in Figure 35d.

D. RELATED EXPERIMENTS

Additional experiments were performed to complete the parametric study of the linear explosive drivers. For example, Figure 36 compares the performance of two explosive drivers in which various masses of diluted nitromethane were used to collapse an 0.316-inch outside diameter by 0.258-inch inside diameter steel tube containing helium at 660 psi. The effects produced by this variation for these conditions are quite small and probably within the experimental uncertainties.

In another experiment the detonation velocity was varied. The shock trajectory of a driver using diluted nitromethane, whose detonation velocity is 5.5 km/sec, turned out to be quite similar to that of one using Composition C-4,
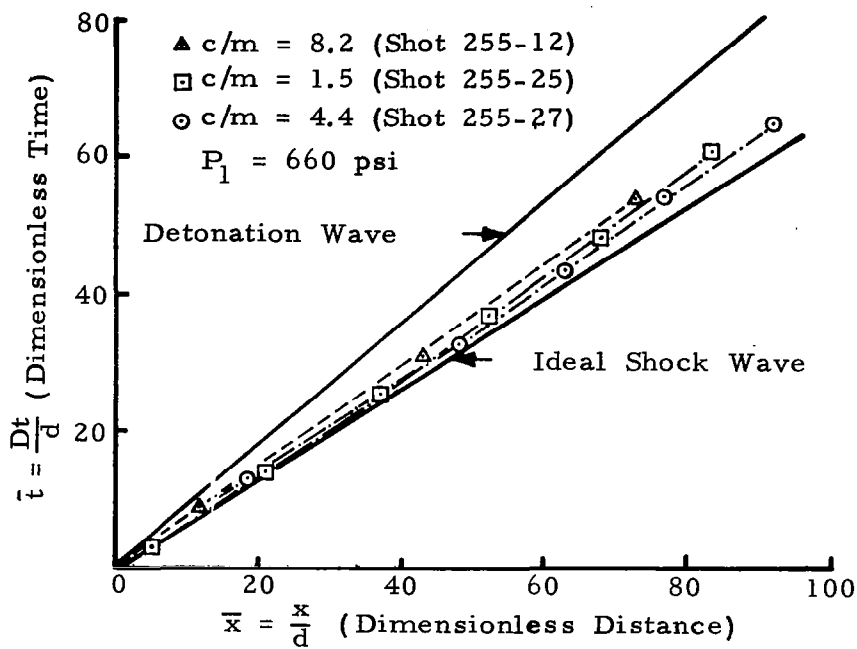
FIGURE 36. A COMPARISON OF SHOCK TRAJECTORIES
PRODUCED BY EXPLOSIVE DRIVERS HAVING
DIFFERENT EXPLOSIVE-TO-PRESSURE-TUBE
MASS RATIOS

whose detonation velocity is 8.6 km/sec. This trajectory comparison is made in Figure 37. The pressure tubes used throughout the experiment were the same: outside diameter = 0.316 in. and inside diameter = 0.258 in., containing helium at 660 psi.

An experiment was designed to determine the scalability of driver performance, in which all driver dimensions were increased by a factor of two. The pressure tube was virtually twice as large as those used in the experiments described above. The initial pressure in the helium was 660 psi. Figure 38 shows that the performance of this diluted-nitromethane driver (Shot 255-17) was at first identical with that of the smaller driver (Shot 255-15). The slightly higher initial shock velocity followed by a gradual deceleration due to the boundary-layer effects was quite scalable.
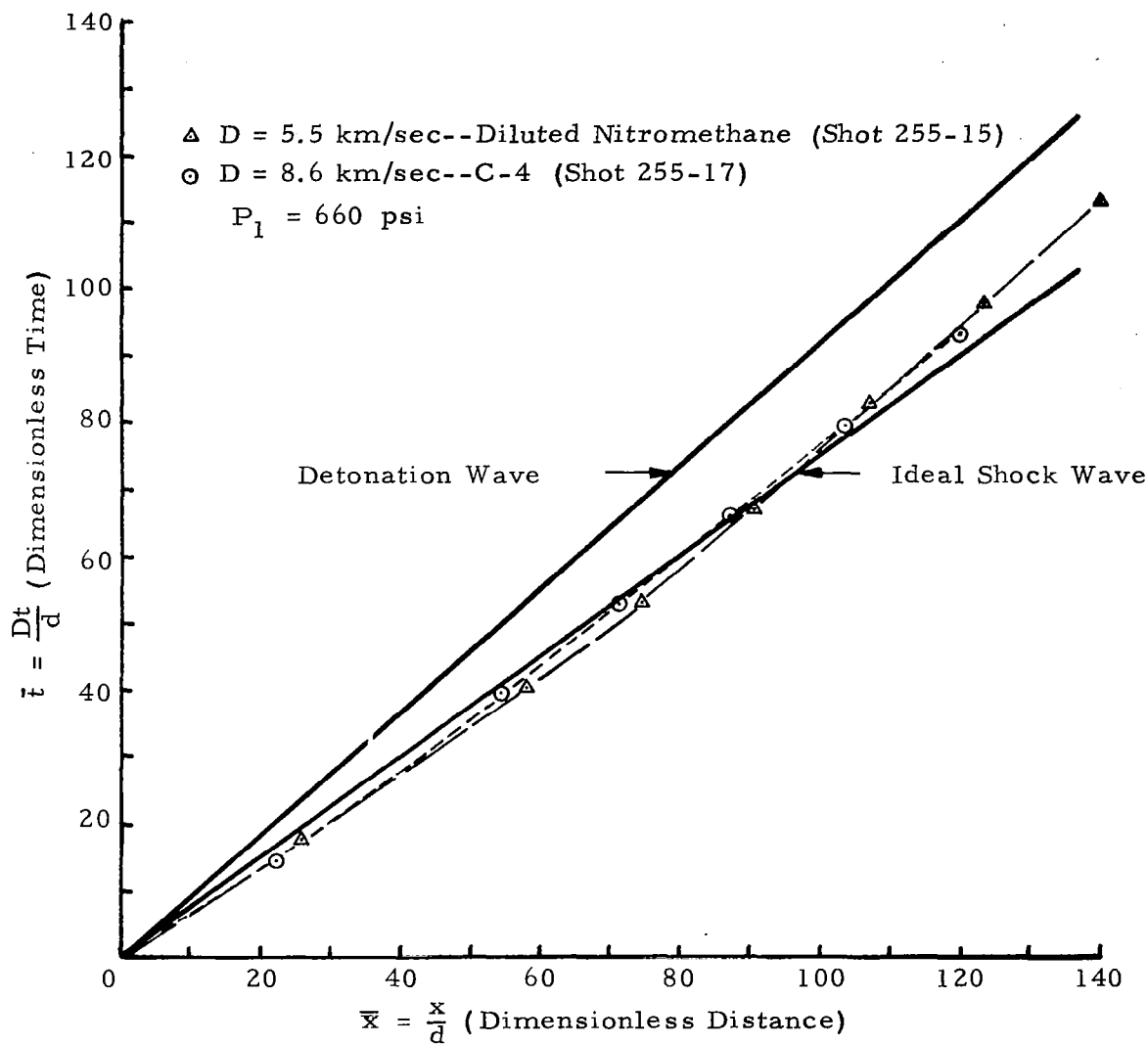
FIGURE 37.   COMPARISON OF EXPLOSIVE DRIVERS USING
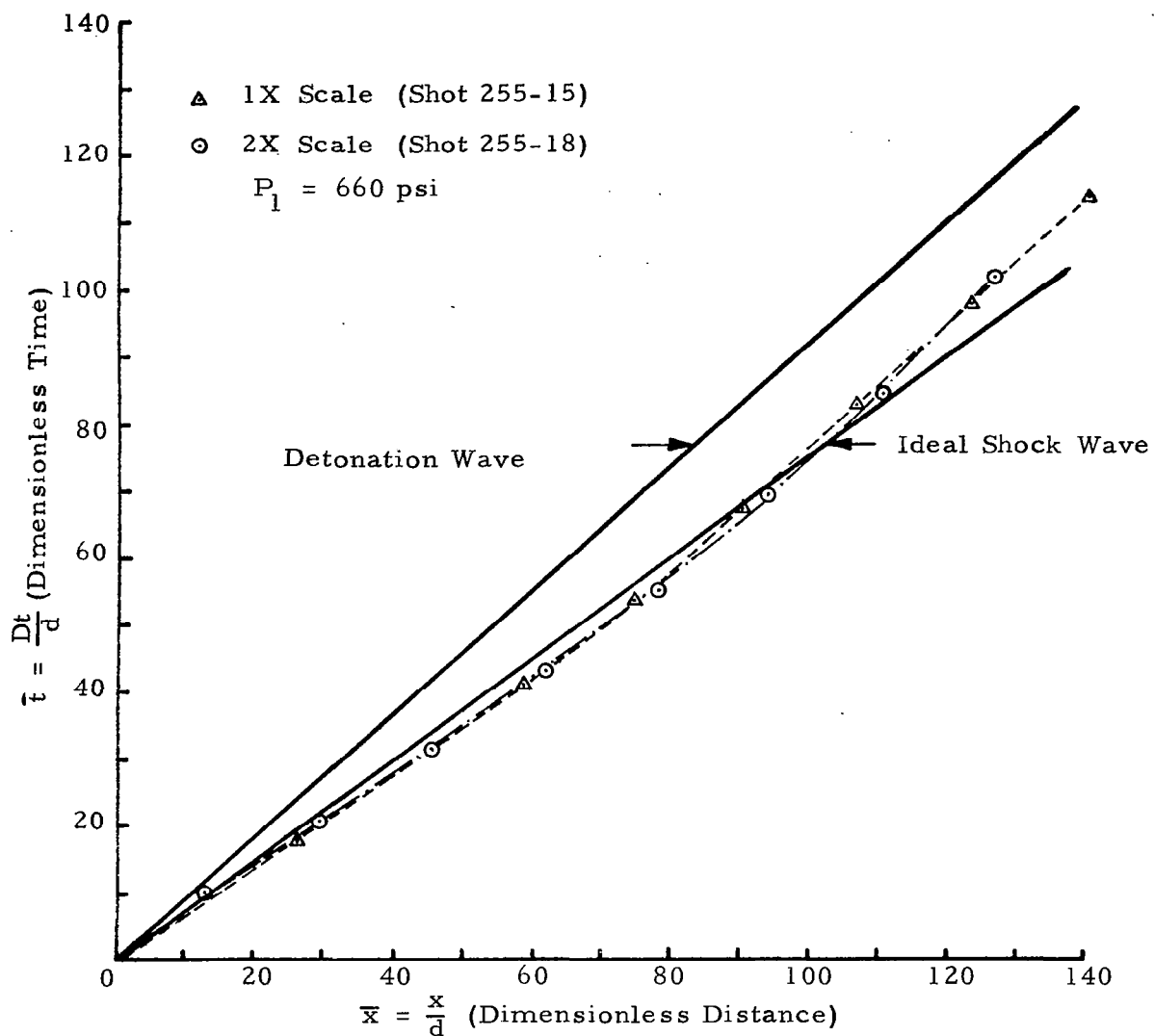DIFFERENT EXPLOSIVES

FIGURE 38. COMPARISON OF SHOCK WAVE TRAJECTORIES
PRODUCED BY A PARTICULAR EXPLOSIVE DRIVER
AND A 2X SCALE-UP OF IT

SECTION V

CONCLUSION

A. SUMMARY

The results of the analytical and experimental investigations conducted during this program have demonstrated the feasibility of using explosively driven launchers to obtain projectile velocities that are significantly higher than those obtainable by conventional launchers. A two-stage, explosively-driven light gas gun has been designed and used to accelerate a 0.17 gm magnesium-lithium projectile to 12.2 km/sec. The operational concepts of the explosive lensing system employed in the second-stage acceleration process have been experimentally verified. Tests have shown that the explosive lens can be used to produce an implosively formed piston whose motion can be accurately programmed.

A comprehensive experimental investigation of explosive drivers produced sufficient data to formulate a model of driver operation which accounts for observed departures from the ideal operation. The model included the effects of boundary layer, jetting, and pressure tube expansion. The calculative techniques used to predict the performance of the two-stage launcher were modified to include these effects.

B. RECOMMENDATION FOR FUTURE WORK

No attempt has been made to optimize the performance of the present launching system or maximize the projectile velocities. Instead, the main effort has been to experimentally determine the basic feasibility of a two-stage launcher using the explosive lensing system. The present inability to launch an intact projectile is a consequence of improper matching of the first-stage gasdynamic cycle with the second-stage acceleration. The uniformly

accelerated second-stage piston tends to trap the projectile in its cone because the pressure in the accelerating gas is insufficient to maintain an adequate distance between the piston and the projectile. The primary objective of future work should be to design and test a complete launcher in which the acceleration of the second stage is matched to the gasdynamic conditions produced by the first stage. Such a launcher would produce an almost constant base-pressure acceleration and eliminate the possibility of trapping the projectile. After an intact projectile has been launched to the previously achieved velocities (12.2 km/sec), the second stage lens should be redesigned to produce even higher projectile velocities until the upper velocity limit of the two-stage launcher system is ultimately determined. Once the velocity range is established, emphasis should be directed toward launching complex shapes such as spheres and cones.

REFERENCES

1. P. B. Archibald, "A Low Density, Low Pressure Solid Explosive," UCRL-14186, University of California, Lawrence Radiation Laboratory, Livermore, California, May 1965.

2. E. T. Moore, Jr., C. S. Godfrey, and H. F. Waldron, "Recent Developments in the Use of Chemical Explosives for Hypervelocity Test Devices." Paper presented at the Fifth Hypervelocity Techniques Symposium, March 16 and 17, 1967, at the Denver Research Institute, Denver University, Denver, Colorado.

3. H. F. Waldron, E. T. Moore, Jr., G. Steel, and C. S. Godfrey, "A Mechanism for the Conversion of the Chemical Energy of Explosives to the Kinetic and Internal Energy of a Gas," AIAA Paper No. 67-178. Presented at the AIAA Fifth Aerospace Meeting, New York, New York, January 1967.

4. H. Mirels, "Shock Tube Test Time Limitation Due to Turbulent-Wall Boundary Layer," AIAA Journal, II, 84 (January 1964).

5. G. Birkhoff, D. P. MacDougall, E. M. Pugh, and G. I. Taylor, "Explosives With Lined Cavities," Journal of Applied Physics, XIX, 563 (June 1948).

6. J. M. Walsh, R. G. Shreffler, and F. J. Willig, "Limiting Conditions for Jet Formation in High Velocity Collisions," Journal of Applied Physics, XXIV, 349 (March 1953).